

AD-A167 072

CORRECTION FOR PROBE-POSITION ERRORS IN PLANAR
NEAR-FIELD SCANNING(U) AIR FORCE INST OF TECH
WRIGHT-PATTERSON AFB OH SCHOOL OF ENGINEERING

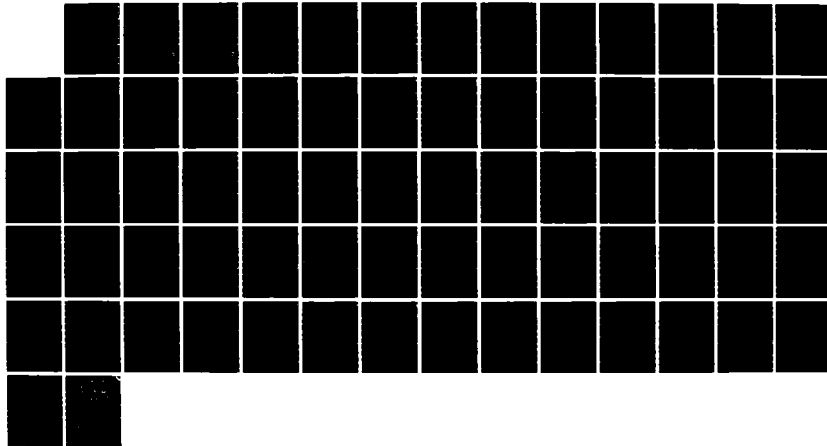
1/1

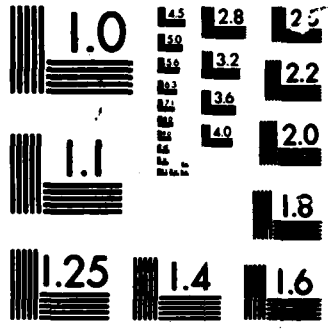
UNCLASSIFIED

D R REDDY DEC 85 AFIT/GE/ENG/85D-34

F/G 14/2

NL





MICROCOPY

CHART

1

AD-A167 072



CORRECTION FOR PROBE-POSITION ERROR
 IN PLANAR, NEAR-FIELD SCANNING
 THESIS
 David R. Reddy
 Second Lieutenant, USAF

DISTRIBUTION STATEMENT A
 Approved for public release
 Distribution Unlimited

DTIC
 ELECTE
 MAY 12 1986
 S
 B

DEPARTMENT OF THE AIR FORCE
 AIR UNIVERSITY

AIR FORCE INSTITUTE OF TECHNOLOGY

Wright-Patterson Air Force Base, Ohio

86 5 12 037

DTIC FILE COPY

AFIT/GE/ENG/85D-34

CORRECTION FOR PROBE-POSITION ERRORS
IN PLANAR, NEAR-FIELD SCANNING
THESIS

David R. Reddy
Second Lieutenant, USAF

AFIT/GE/ENG/85D-34

DTIC
ELECTE
MAY 12 1986
S D
B

Approved for public release; distribution unlimited

AFIT/GE/ENG/85D-34

**CORRECTION FOR PROBE-POSITION ERRORS
IN PLANAR, NEAR-FIELD SCANNING**

THESIS

**Presented to the faculty of the School of Engineering
of the Air Force Institute of Technology**

Air University

**In Partial Fulfillment of the
Requirements for the Degree of
Master of Science in Electrical Engineering**

**David R. Reddy, B.S.
Second Lieutenant, USAF**

December 1985

Approved for public release; distribution unlimited

Preface

This paper applies the simple Taylor series approximation to the intricate problem of correcting inaccurate probe-positioning in planar, near-field scanning.

This is not to imply that the implementation is as simple as the concept. Throughout the past eight months I have learned that simple concepts can be quite difficult to implement.

There are many subtleties that the student new to this area encounters. Dealing with the minor differences between todays modern main-frame computers alone can delay indefinitely the more improtant development and interpretation of the computer analysis.

There are several individuals who helped me overcome these differences. Particular thanks goes to my sponsor, Dr. Arthur D. Yaghjian, RADC/EEC, Hanscom AFB. Without his help this thesis would not have been possible. Thanks also goes to my thesis advisor, 1Lt Randy Jost, for his guidance and patience to the point of correcting my spelling mistakes.

Finally, I would like to acknowledge Allen C. Newell, of the National Bureau of Standards, as the one who first proposed this method of probe position compensation.

<input checked="" type="checkbox"/>
<input type="checkbox"/>
<input type="checkbox"/>

by	
Distribution/	
Availability Codes	
Dist	Avail and/or Special
A-1	

Table of Contents

	page
Preface	ii
List of Figures	iv
Abstract	v
I. Introduction	1
II. Theoretical Development	4
III. The Database	11
General Outline	12
Near-Field Computation	14
The Subroutine Fact	14
The Subroutine FacFact	15
The Subroutine Sphebe	15
The Subroutine Legend	16
The Main Program	16
IV. The Transformation Routines	18
Program Descriptions	20
TRPROG	20
DRPROG	23
COMPROG	24
OUTPROG	24
Positioning Error Simulation	25
V. The Data	28
The Model	28
Computation Procedure	29
Data Presentation	30
Evaluation of the Programs	38
VI. Results and Recommendations	40
Appendix A: Program Listings	42
Bibliography	58
Vita	60

List of Figures

Figure	page
1. Hypothetical Test Antenna Geometry	12
2. Block Diagram of Computation Procedure	19
3. The Coordinate Transformation Process	21
4. Modeled Probe Positioning Errors	26
5. Computation Procedure for Data Presentation	29
6. Perfect Scan Pattern vs. Uncorrected Pattern $\Delta z = \lambda / 25$	30
7. Perfect Scan Pattern vs. Corrected Pattern $\Delta z = \lambda / 25$	31
8. Perfect Scan Pattern vs. Uncorrected Pattern $\Delta z = \lambda / 10$	32
9. Perfect Scan Pattern vs. Corrected Pattern $\Delta z = \lambda / 10$	33
10. Near-Field Phase, Uncorrected Scan $\Delta z = \lambda / 10$	34
11. Near-field Phase, Corrected Scan $\Delta z = \lambda / 10$	35
12. Near-Field Magnitude, Uncorrected Scan $\Delta z = \lambda / 10$	36
13. Near-Field Magnitude, Corrected Scan $\Delta z = \lambda / 10$	37

Abstract

In recent years, near-field antenna measurement techniques have gained a good deal of acceptance. There are several errors in the computed far-field patterns caused by measurement inaccuracies in the near-field data. This paper deals with deterministic errors introduced by probe-positioning errors in planar, near-field scanning.

By utilizing basic near-field theory, as well as a knowledge of the positioning errors, it is possible to estimate the fields at the correct probe position. A computer program which lessens the effect of probe positioning errors by means of a truncated Taylor series expansion is used to demonstrate this improvement.

To simulate inaccurate probe positioning, a database of calculated near-field values for a linearly polarized, uniformly illuminated, circular aperture was used. Next, the position correction program was applied to computer generated inaccurate data. Finally, far-field patterns were calculated, and compared using both the corrected and uncorrected data. Results of the comparisons are presented. Limitations, and areas of application of this routine are discussed.

I. INTRODUCTION

Background

Near-field scanning techniques are quickly becoming accepted as an efficient, and accurate method for the determination of antenna patterns [9:492]. Near-field techniques offer many advantages over conventional antenna measurement facilities including: all weather operation, reduced ambient interference, and security for delicate, or classified apparatus [11:101]. To further enhance the reliability of antenna parameters predicted by this procedure, any source of error must be acknowledged and limited where possible.

Near-field scanning requires the measurement of probe output, in both phase and magnitude, over a predetermined scanning surface such as a sphere, circular cylinder, or plane [7]. This is accomplished by positioning a probe at a point on the scanning surface through the use of mechanical devices. Since mechanical devices, such as positioners, are not infinitely accurate, some error in the probe positioning exists. Inaccurate probe position specification leads to erroneous far-field patterns, calculated from the incorrect data gathered by the probe.

Problem Statement

This thesis will examine sensitivity to inaccurate probe positioning, as well as a possible method for reducing

that sensitivity by means of a truncated Taylor series approximation of the near-field data.

Scope

A computer program, created to generate the near-field, transverse electromagnetic fields on a plane in front of the antenna is used as a data base for the computation of far-field antenna patterns. Inaccuracies in probe positioning are simulated by the manipulation of this program. This data set is used to calculate the far-field pattern of the test antenna using planar scanning techniques explained in Chapter II. The resulting pattern is then compared to the pattern from a perfect scan for various degrees of inaccurate positioning.

Also, the position correction routine is used to compensate for erroneous probe positioning and again the far-field pattern is calculated. This "corrected" pattern is compared to the uncorrected pattern as well as the pattern from the perfect scan, to determine whether or not any improvement has occurred. This procedure is also repeated for various degrees of positioning error.

Assumptions

To lessen the number of the computations, and to conserve computer time, two assumptions are made:

- 1) The simulated positioning errors are discrete in nature, and consist of a single displacement at the center line of the scanning surface.

2) The hypothetical probe used is an ideal electric dipole sampling the electric fields.

General Approach

This research effort began with a review of the development and theoretical formulation of planar, near-field scanning techniques. The results of this review that are pertinent to this presentation are given in Chapter II.

After an understanding of the basic theory of planar, near-field scanning was obtained, a data base of near-field values was needed to investigate the effect of probe positioning errors. A computer program that calculates the fields of a circular aperture, linearly polarized antenna as a function of frequency, aperture radius, and distance from the antenna was used to generate this data. A description of that program is presented in Chapter III.

Next, a program which calculates the far-field pattern of an antenna from its near-field values was created to examine the effect of inaccurate probe positioning. The position correction routine is an integral portion of this program. Both procedures are explained in detail in Chapter IV.

Finally, the effect of positioning errors, as well as the effectiveness of the position correction routine in limiting these errors is examined through a computer analysis of the far-field patterns produced. This analysis, and the results it provided are presented in Chapter V.

II. THEORETICAL DEVELOPMENT

In this chapter, the basic theory behind planar, near-field measurements is developed. The definitive analysis in this area was performed by D. M. Kerns [12]. The approach used involves the expansion of a set of measured field values into a summation of its elementary, planar wave functions.

The following is a list of the variables and the notations that will be used throughout the theoretical development of this report.

$\overline{E}(\overline{r})$ = The electric field, magnitude and phase of each component, as a function of position.

$\overline{A}(\overline{k})$ = The vector amplitude, magnitude and phase of each component, as a function of propagation direction.

\overline{r} = The position vector $x \hat{a}_x + y \hat{a}_y + z \hat{a}_z$.

\overline{k} = The propagation vector $k_x \hat{a}_x + k_y \hat{a}_y + k_z \hat{a}_z$.

ω = The frequency in rad/sec.

ϵ = The permittivity of the propagation medium.

μ = The permeability of the propagation medium.

\overline{R} = The tangential position vector $x \hat{a}_x + y \hat{a}_y$.

\overline{K} = The tangential direction vector $k_x \hat{a}_x + k_y \hat{a}_y$.

\overline{dK} = The two dimensional elemental patch in k-space, $dk_x dk_y$.

\overline{dR} = The two dimensional elemental patch in real space, $dx dy$.

k = The phase propagation constant $2\pi/\lambda$.

\overline{k}_0 = $k \hat{a}_r$.

The propagation of electromagnetic waves within free-space is described by Maxwell's equations. These equations lead directly to the vector Helmholtz equation [13:124].

$$\nabla^2 \bar{E}(\bar{r}) + k^2 \bar{E}(\bar{r}) = 0 \quad (1)$$

The simplest, non-trivial solution to equation (1) for a homogeneous, isotropic, source free region ($z > 0$) is given by [1:145]:

$$\bar{E}(\bar{r}) = \bar{A}(\bar{k}) e^{-i \bar{k} \cdot \bar{r}} \quad (2)$$

where: \bar{r} is the position vector
 \bar{k} is the direction of propagation
 $\bar{A}(\bar{k})$ is the vector amplitude of the wave as a function of the direction of propagation.

By substituting equation (2) into equation (1), we obtain [1:144]:

$$k_x^2 + k_y^2 + k_z^2 = k^2 \quad (3)$$

An interesting property of equation (3) is that given two components of the propagation vector, say k_x and k_y , the third component, k_z , is specified.

$$k_x^2 + k_y^2 + k_z^2 = \omega^2 \mu \epsilon \quad (4)$$

All values of k_x , and k_y which yield a real value for k_z define the propagating modes. However, modes for which equation (4) produces a complex result are evanescent, or

non-propagating. Still these evanescent modes must satisfy the convergence condition, namely [5:374]:

$$\lim_{r \rightarrow \infty} \bar{A}(\bar{k}) e^{-i \mathbf{k} \cdot \bar{r}} = 0 \quad (5)$$

It is for this reason that we choose the following [1:146; 10:499]:

$$k_z = \begin{cases} \sqrt{k^2 - K^2} & K^2 \leq k^2 \\ -i \sqrt{K^2 - k^2} & K^2 > k^2 \end{cases} \quad (6)$$

Note that k_z is either positive real, or negative imaginary.

Since we have assumed a source free region, Maxwell's equations require that [13:112]:

$$\nabla \cdot \bar{E}(\bar{r}) = 0 \quad (7)$$

substituting equation (2) into equation (7) yields:

$$\bar{k} \cdot \bar{A}(\bar{k}) = 0 \quad (8)$$

Equation (8) implies that given the direction of propagation, and two components of the vector amplitude, the third component is uniquely defined as:

$$A_z = \frac{-1}{k_z} (A_x k_x + A_y k_y) \quad (9)$$

For any complex system, the complete electric field, at any point in the source free region, can be expressed as a

summation of the elementary wave functions over all possible propagation directions [5:374; 15].

$$\bar{E}(\bar{r}) = \frac{1}{2\pi} \int_{-\infty}^{\infty} \int_{-\infty}^{\infty} \bar{A}(\bar{k}) e^{-i \bar{k} \cdot \bar{r}} d\bar{K} \quad (10)$$

If $\bar{A}(\bar{k})$ in equation (10) is expressed in rectangular components, the integral can be reduced to three scalar expressions, corresponding to each of the unit vector components.

$$E_x = \frac{1}{2\pi} \int_{-\infty}^{\infty} \int_{-\infty}^{\infty} A_x e^{-i \bar{k} \cdot \bar{r}} d\bar{K}$$

$$E_y = \frac{1}{2\pi} \int_{-\infty}^{\infty} \int_{-\infty}^{\infty} A_y e^{-i \bar{k} \cdot \bar{r}} d\bar{K} \quad (11)$$

$$E_z = \frac{1}{2\pi} \int_{-\infty}^{\infty} \int_{-\infty}^{\infty} A_z e^{-i \bar{k} \cdot \bar{r}} d\bar{K}$$

A closer examination of the integral expressions given in equation (11) reveals that they are the two dimensional Fourier transforms of the components of $\bar{A}(\bar{k})$ [4:381]. The inverse relation is given by [5:375; 15]:

$$\bar{A}(\bar{k}) = \frac{1}{2\pi} \int_{-\infty}^{\infty} \int_{-\infty}^{\infty} \bar{E}(\bar{r}) e^{+i \bar{k} \cdot \bar{r}} d\bar{R} \quad (12)$$

By specifying the x and y components of the electric field over a plane defined by $z=z_0$ we can determine from equation 12 the x and y components of $\bar{A}(\bar{k})$, and by using equation (9) we can uniquely specify the remaining component A_z .

$$A_x = \frac{1}{2\pi} \int_{-\infty}^{\infty} \int_{-\infty}^{\infty} E_x e^{+i \bar{k} \cdot \bar{r}} d\bar{R}$$

$$A_y = \frac{1}{2\pi} \int_{-\infty}^{\infty} \int_{-\infty}^{\infty} E_y e^{+i \bar{k} \cdot \bar{r}} d\bar{R}$$
(13)

Given $\bar{A}(\bar{k})$, the electric field is known for all space by equation (10). Generally, this equation must be performed on a computer. However, for the case of the far-field pattern, equation (10) can be evaluated analytically using the method of steepest descent [5:375; 3:1675; 6:253].

$$\bar{E}_{FF}(\bar{r}) = i 2\pi k_{z0} \bar{A}(\bar{k}_0) \frac{e^{-i(kr)}}{r}$$
(14)

where: $\bar{k}_0 = k \hat{a}_r$
 $\hat{a}_r = \sin(\theta) \cos(\phi) \hat{x} + \sin(\theta) \sin(\phi) \hat{y} + \cos(\theta) \hat{z}$
 Finally, note that since $k_{x0}^2 + k_{y0}^2 = k^2 \sin^2(\theta) < k^2$
 equation (14) involves only the spectrum of the propagating modes.

Probe Positioning Errors

The foregoing development assumed that the tangential field was known over a plane defined by $z=z_0$. It is impossible to create a perfect measuring apparatus, therefore some error is always present in the form of inaccurate probe positioning. This error can occur in two distinct forms:

1. Random error introduced by loose machinery, temperature variations, or ground vibrations.

2. Deterministic positioning errors due to limited machine accuracy.

The first is time variant, and can be eliminated by making a statistical average of several scans. For a given system, the deterministic errors can be measured with greater accuracy than the positioning machinery is capable of achieving, and it is this type of positioning error that is the topic of this investigation.

The deviation of the probe from the theoretical plane of measurement will introduce errors in the far-field patterns. To counter this we will use the spatial deviation measured and a knowledge of the dependence of the tangential fields on variations in the z direction to estimate the value of the fields at the theoretical plane of measurement. We will consider errors in the z direction only.

To estimate the value of the tangential electric fields, we will make use of a truncated Taylor series expansion. The general form of the Taylor series is given by [18, 305]:

$$F(z) = \sum_{n=0}^{\infty} \frac{1}{n!} \frac{d^{(n)}}{dz^{(n)}} \Big|_{z=z_0} F(z) (z-z_0)^n \quad (15)$$

If we assume that the higher orders of the series are dominated by the first and second terms we can say:

$$\bar{E}(z) = \bar{E}(z_0) + \frac{d}{dz} \left[\bar{E}(z) \right]_{z=z_0} \Delta z \quad (16)$$

By examining equation (10) we can see that:

$$\frac{d}{dz} [\bar{E}(z)]_{z=z_0} = \frac{1}{2\pi} \int_{-\infty}^{\infty} \int_{-\infty}^{\infty} (-iK_z) \bar{A}(\bar{k}) e^{-i\bar{k} \cdot \bar{r}_0} d\bar{k} \quad (17)$$

$$\bar{r}_0 = x\hat{a}_x + y\hat{a}_y + z_0\hat{a}_z$$

So, if we knew the vector amplitude function of a perfect scan, $\bar{A}(\bar{k})$, we could determine the first partial of the electric field with respect to z and approximate the value of the fields on the plane $z=z_0$. $\bar{A}(\bar{k})$ is not yet known, but we can approximate $\bar{A}(\bar{k})$ by using equation (13) to calculate a $\bar{A}_0(\bar{k})$ which is the vector amplitude function calculated using the measured data, and neglecting the positioning errors.

$$\bar{A}_0(\bar{k}) = \frac{1}{2\pi} \int_{-\infty}^{\infty} \int_{-\infty}^{\infty} \bar{E}(z_1) e^{+i\bar{k} \cdot \bar{r}_0} d\bar{R} \quad (18)$$

Therefore, our equation for the tangential fields on the theoretical plane of measurement becomes [17:24]:

$$\bar{E}(z_0) = \bar{E}(z_1) - \frac{\Delta z}{2\pi} \int_{-\infty}^{\infty} \int_{-\infty}^{\infty} (-iK_z) \bar{A}_0(\bar{k}) e^{-\bar{k} \cdot \bar{r}_0} d\bar{K} \quad (19)$$

In general, $\Delta z = (z_1 - z_0)$ is dependent on the x, y coordinates of the point in question.

III. THE DATABASE

Before a study into probe positioning errors can begin, a database of near-field electric field values along with their accompanying far-field patterns must be obtained. For this investigation, the database must include flexibility of the positioning discrepancies as well as a reliable degree of accuracy so as not to mask the outcome of any correcting routines used. Finally, since the database will be accessed repeatedly, it should be as easy to use as possible.

For these reasons, a computer program that calculates the tangential electric fields in the near-field of a linearly polarized, uniformly illuminated, circular aperture antenna was chosen as a source of raw data over actual measurements. The original analysis and program was written by Dr. Arthur Yaghjian RADC/EEC, Hanscom AFB, and provides data based on parameters supplied by the user. The main parameters are, ka (i.e. $2\pi a/\lambda$) and z/a where z is the distance to the plane of computation.

General Outline

To create the database program, the fields of the test antenna were expanded into elementary spherical harmonics [8]. This was accomplished by first examining the corresponding acoustical problem of the two-sided piston radiator. Since the differential equations of acoustics are only slightly different from those governing electromagnetics, similar radiating systems yield similar results. By expanding the acoustical pressure pattern of the two-sided piston radiator into spherical harmonics, an expression is obtained that can be used as a starting point for the more difficult electromagnetics problem. This process leads to an equation that is an infinite sum of individual spherical modes, an equation that lends itself to computation by computer.

The geometry that the database program is based on is given in figure 1.

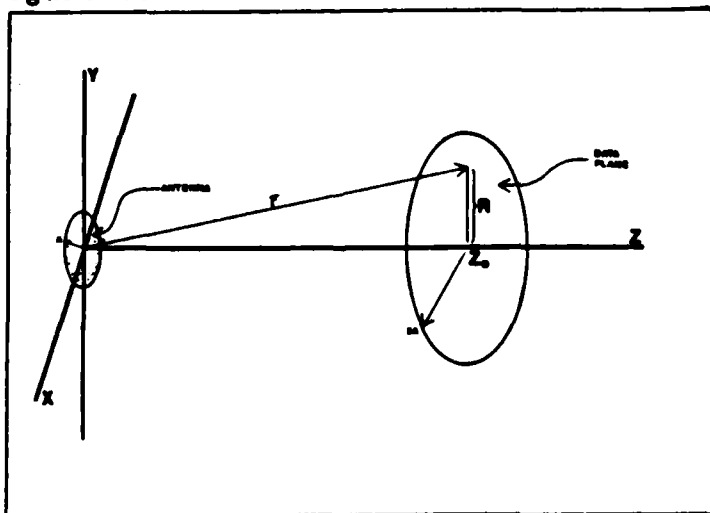


Figure 1. Hypothetical Test Antenna Geometry.

The equation which yields the electric field values for all points outside the source sphere (i.e. $|\bar{r}| > a$) is given by [8:13]:

$$\frac{E_x(r)}{2E_0} = \frac{-(ka)^2}{2ikr} \sum_{\substack{l=0 \\ \text{even}}}^{\infty} B_l \left[(l+1) (\cos\theta P_l - P_{l+1}) h_l^{(2)} + \cos\theta (lh_l^{(2)} - kr h_{l+1}^{(2)}) P_l \right]$$

$$B_l = \frac{(2l+1)}{2^{l+1}} \sum_{q=1}^{l/2} \left(\frac{(l-1-2q)!!(l-1+2q)!!(-1)^{\frac{l}{2}+q}}{(\frac{l}{2}-q)! (\frac{l}{2}+q)!} \right) \times \left(jq \left(\frac{ka}{2}\right)_{j-q} \left(\frac{k\phi}{2}\right) + \left(\frac{(l-1)!!}{(\frac{l}{2})!} J_0\left(\frac{ka}{2}\right) \right)^2 (-1)^{\frac{l}{2}} \right) \quad (20)$$

Note that all of the summation constants, B_l , are real. Therefore the phase information is given by expressing the Hankel functions as:

$$h_n^{(2)} = j_n(x) - i n_n(x) \quad (21)$$

At first glance it would appear that this equation would supply both the near-field values, and the far-field values. Practically, this is not the case due to the fact that as the computation surface is moved away from the test antenna, the number of terms needed to insure accuracy becomes prohibitively large. Fortunately, this is not a

problem since the far-field pattern of this system can be expressed in closed form. The far-field pattern is given by [2:417]:

$$\left| \frac{E(\theta)}{E_0} \right| = \frac{2 J_1(ka \sin\theta)}{ka \sin\theta} \quad (22)$$

Near-Field Computation

The near-field database program addresses each component of equation (20) separately. There are, however, four special functions that are common through out the computational procedure of a single data set. These special functions are calculated in subroutines called by the main program and they include:

- 1) The Factorial Function
Calculated in the subroutine Fact
- 2) The Fac-Factorial Function
Calculated in the subroutine Facfact
- 3) The Spherical Bessel Functions
Calculated in the subroutine Sphebe
- 4) The Legendre Polynomial Functions
Calculated in the subroutine Legend.

Each subroutine is governed by recurrence relations that define the special function that it calculates.

The Subroutine Fact

This subroutine is a simple algorithm that calculates the factorials of the first N integers where N is a limiting value supplied by the main program. The equation used to

calculate these values is given by:

$$P! = \prod_{n=1}^P n \quad (0! \equiv 1) \quad (23)$$

The Subroutine Facfact

This routine calculated the double factorials of the first $2N+1$ integers where N is a maximum value supplied by the main program, and is based on the parameters supplied by the user. The expression used to calculate these values is given by:

$$(2P+1)!! = \prod_{n=1}^P (2n+1) \quad (24)$$

The Subroutine Sphebe

This routine is slightly more complex than the preceding two, since it must calculate the spherical Bessel functions of an arbitrary order and arbitrary arguments. That is, it must calculate the ordinary spherical Bessel functions as well as the spherical Neumann functions. The equation used is:

$$f_{n-1}(x) + f_{n+1}(x) = \frac{2n+1}{x} f_n(x) \quad (25)$$

All cases use known forms of $j_n(x)$ and $n_n(x)$ or the above recurrence relation.

For $j_n(x)$ we use a descending computation starting at $N > n$ and set $j_N(x) = 0$, $j_{N-1}(x) = \delta$, $|\delta| \ll 1$

For $n_n(x)$ we use an ascending computation using the

known forms of the first two Neuman functions.

The Subroutine Legend

This routine calculates the Legendre Polynomials up to order N , and for argument $\cos(\theta)$, where N , and $\cos(\theta)$ are provided by the main program. The algorithm is based on the equations:

$$(2n+1) x P_{(n)}(x) = (n+1) P_{(n+1)}(x) + n P_{(n-1)}(x)$$

$$P_0 (\cos\theta) = 1 \tag{26}$$

$$P_1 (\cos\theta) = \cos\theta$$

The Main Program

The main program begins calculation of field values by first calculating the summation constants B_l given in equation (20). Next, the program calculates the phase and magnitude of the fields. This is done by taking full advantage of the radial symmetry of the geometry. Examining equation (22), it is noted that the far-field pattern is symmetric about the z -axis. Therefore, the program only needs to calculate the near-field values on any ray normal to the z -axis, and lying in the plane of computation. This reduces the number of values to be calculated and the time of computation.

The main program introduces a variable R , which is the distance off of the bore sight of the antenna on the plane of computation. It then calculates the phase and magnitude of the electric field at that point. The equation for

these values is given by [8:15]:

$$I_m \left(\frac{E_x(\bar{r})}{2 E_0} \right) = \frac{+(ka)^2}{2kr} \sum_{\substack{\ell=0 \\ \text{even}}}^{\infty} B_\ell \left| (\ell + 1) (\cos\theta P_\ell - P_{\ell+1}) j_\ell(kr) \right. \\ \left. + \cos\theta (\ell j_\ell(kr) - kr j_{(\ell+1)}(kr) P_\ell) \right|$$

$$R_e \left(\frac{E_x(\bar{r})}{2 E_0} \right) = \frac{-(ka)^2}{2kr} \sum_{\substack{\ell=0 \\ \text{even}}}^{\infty} B_\ell \left| (\ell + 1) (\cos\theta P_\ell - P_{\ell+1}) n_\ell(kr) \right. \\ \left. + \cos\theta (\ell n_\ell(kr) - kr n_{(\ell+1)}(kr) P_\ell) \right| \quad (27)$$

$$\text{Magnitude} = \sqrt{R_e^2 + I_m^2}$$

$$\text{Phase} = \text{Tan}^{-1} \left(\frac{I_m}{R_e} \right)$$

Finally, the program writes these values to a data file which is used as the input data to the Far-Field Transformation Program.

IV. THE TRANSFORMATION ROUTINES

Once a database of unprocessed values has been obtained for the test antenna, the next step is to create programs which reduce this data into a form suitable for comparison. This is accomplished through Transformation Routines.

These programs use the near-field values calculated in the database program to compute the vector amplitude function, $\bar{A}(\bar{k})$ through a numerical evaluation of equation (13). This data is then used to evaluate equation (17) which yields the first partial derivative of the electric field with respect to the variable z , at the plane of measurement. Next, the original near-field data is combined with its first partial by implementing equation (19) and the vector amplitude function is recalculated using this corrected data set. Finally, the far-field pattern is plotted as a function of θ , and compared to the pattern calculated from a perfect scan. Figure 2 is a block diagram of this procedure.

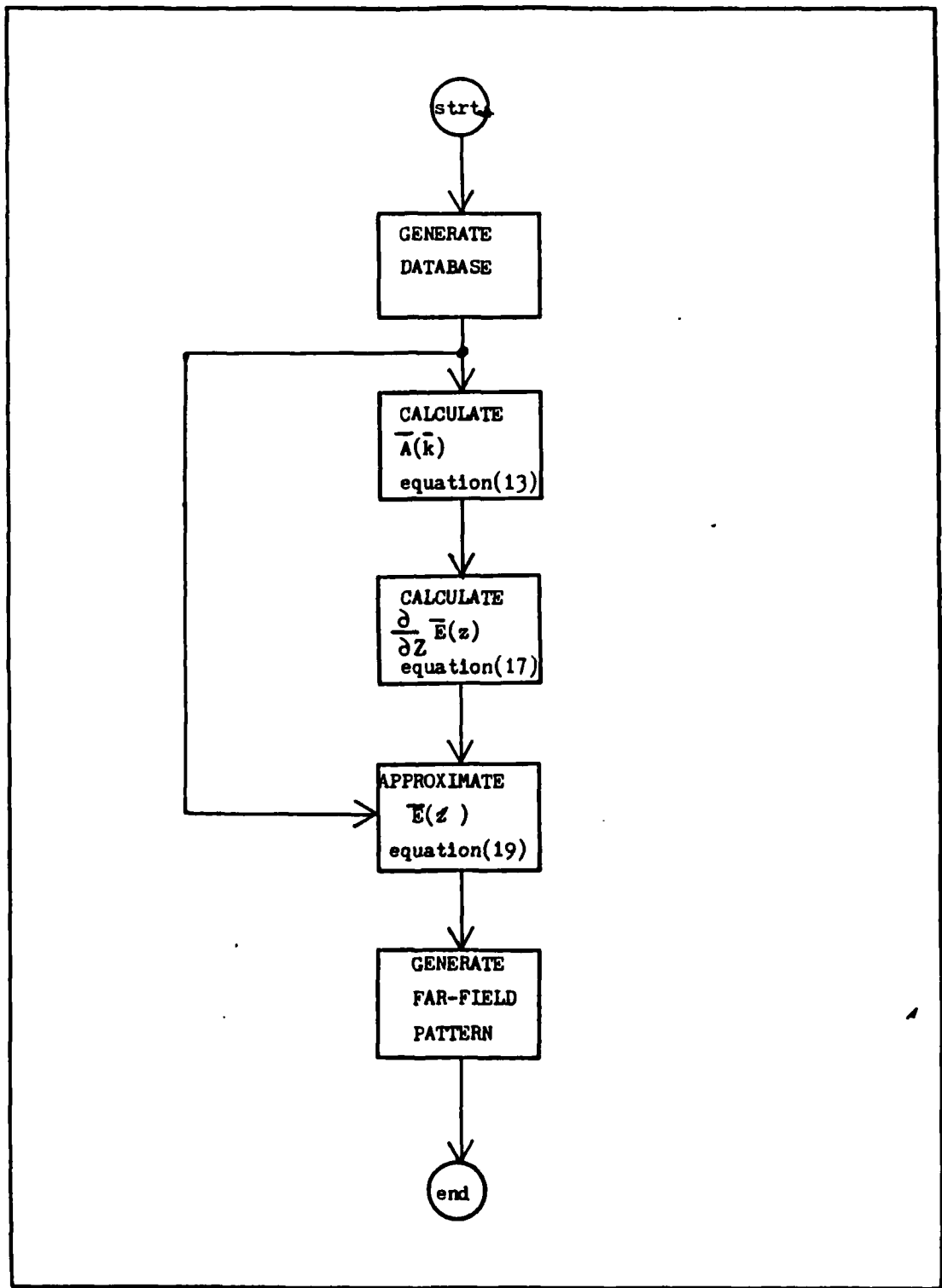


Figure 2. Block Diagram of Computation Procedure.

Program Descriptions

The process depicted in figure 2 is performed in four steps. This is necessary due to hardware limitations on the maximum job size presented by the main frame computer used. Each step represents a separate computer program, and each program evaluates one of the equations outlined in Figure 2. The programs, in order of operation, are:

- 1) The Transformation Program, TRPROG
- 2) The Derivative Program, DRPROG
- 3) The Combination Program, COMPROG
- 4) The Output Program, OUTPROG

The following is a detailed description of each program.

TRPROG

This program evaluates equation (13) by first reading in the near-field data, and then performing the double integral for each point in the transform space (K-space) where a value for the vector amplitude function is required.

There is a complication in reading the near-field values supplied by the database. As described in Chapter II, the database program calculates the near-field values for a linearly polarized, uniformly illuminated, circular aperture antenna. It accomplishes this taking full advantage of the cylindrical symmetry of the problem. Consequently, the final output of the program is in cylindrical coordinates. Before this data can be used by the TRPROG, it must be expressed in cartesian coordinates.

To achieve this, the program first creates a two dimensional array into which the data is to be read. This array represents a scanning plane, and each storage location has associated with it, a pair of cartesian coordinates (x_i, y_i) . Next, TRPROG reads the cylindrical data from the database and stores it in two one-dimensional arrays, one for the phase, and one for the magnitude. Each storage location of the one dimensional arrays has a radial coordinate associated with it. Since the electric field of the test antenna is circularly symmetric about the z-axis, only the radial component is required to specify the field values for a given location. Finally, using the cartesian coordinates associated with each storage location, the radial distance is calculated. The phase and magnitude values from the database whose associated radial dimension most closely matches this calculated radial dimension is read into the storage location as a complex value, see figure 3.

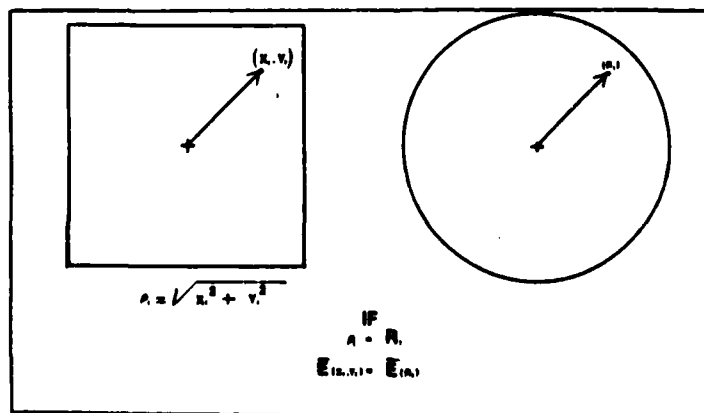


Figure 3. The Coordinate Transformation Process.

After the near-field data has been read, TRPROG performs the double integration of equation (13). This entails a double integral for each value of the vector amplitude function to be calculated. If one examines equation (17), the next equation to be implemented, it is evident that a plane of vector amplitude values will be required for the next computation. This determines which vector amplitude values must be calculated in TRPROG. The simplest, and most direct method of computation is to create a two dimensional array similar to that containing the near-field data and associate each storage location with a pair of coordinates from K-space.

Computation time is a major concern in choosing a method for calculating the double integrals of equation (13). If one simply uses a double summation over all of the near-field data for each K-space point the computer time quickly becomes exceedingly large. Another less time consuming method is to create an intermediate step in the calculation. This requires two loops, the first sums over one of the near-field coordinates for each value of the remaining near-field coordinate, and for each value of one of the K-space coordinates. The second loop sums over the remaining near-field coordinate for each K-space coordinate pair [15; 4:381].

$$\begin{aligned}
 S(y_m, k_x) &= \sum_n E(x_n, y_m) e^{(+ik_x x_n)} \\
 A(k_x, k_y) &= \frac{e^{(+ik_z z_0)} dx dy}{2\pi} \sum_m S(y_m, k_x) e^{(+ik_y y_m)} \quad (28)
 \end{aligned}$$

This method of numerical integration is analagous to taking the one dimensional Fourier Transform of the x variable for each value of y, and then taking the one dimensional Fourier Transform of the y variable for each value of k_x [14:118; 1:75; 7]. The last function of TRPROG is to load the calculated vector amplitude values into a data file for retrieval by the DRPROG.

DRPROG

This program calculates the first partial of the electric field with respect to z by implementing equation (17). The values of the vector amplitude function calculated by TRPROG are read into a two dimensional array. Since the coordinate transformations were performed in TRPROG this is a considerably easier task. Next, the double integral of equation (17) must be computed. A method very similar to that used in the previous program is used.

Again, an intermediate step is introduced into the computation. The first loop sums over all values of one of the K-space coordinates for each value of its real space counter-part, and for each value of the unused K-space coordinate. The second loop sums over all values of the remaining K-space coordinate for each value of its real space counter-part, and for each value of the first K-space

coordinate used [15].

$$\begin{aligned} S(k_{ym}, x) &= \sum_n A(k_{xn}, k_{ym}) e^{-ik_{znm}z_0'} e^{-ik_{xn}x} \\ E(x, y) &= \frac{dk_x dk_y}{2\pi} \sum_m S(k_{ym}, x) e^{-ik_{ym}y} \end{aligned} \quad (29)$$

The major difference between DRPROG and TRPROG is that DRPROG will only sum over the vector amplitude values of propagating modes, because the evanescent modes of the hypothetical test antenna are assumed negligible at $z = z_0 > a$ in front of the aperture.

COMPROG

The combination program evaluates equation (19). It is an extremely simple routine which is separated only to accommodate the hardware limitations discussed previously. Also, to reduce the need for large storage blocks, the near-field data originally read into TRPROG, is re-read into COMPROG.

OUTPROG

The output program re-calculates equation (13). At first glance it would appear that needless programming went into the creation of OUTPROG, however there is one major difference between TRPROG, and OUTPROG. TRPROG, by necessity, calculated the vector amplitude function for a grid of points, equidistant from each other, in K-space. This format, however, is not conducive to presentation as a graph. The vector amplitude, or far-field, pattern is usually presented as a function of the spherical, angular

coordinates θ , and ϕ . Therefore, OUTPROG calculates the vector amplitude function for points equidistant in spherical coordinates. Also, there is no need to calculate a complete grid of data, as a single cut in the θ direction for a fixed value of ϕ will yield all of the information required for comparison. This is due to the fact that the far-field pattern of the test antenna is circularly symmetric.

OUTPROG calculates vector amplitude values for $\phi = \pi/4$ and theta ranging from -30° to $+30^\circ$ in increments of $1/3^\circ$, equation (14) gives the functional relationship between the K vector and θ and ϕ . The computation portion of OUTPROG is identical to TRPROG.

Positioning Error Simulation

To simulate errors in the positioning of a probe, a slight modification is made in the data read by TRPROG. Two sets of near-field values are calculated by the database program. One is a slight distance in front of the theoretical plane of measurement and the other is a slight distance behind the theoretical plane of measurement. As long as the x coordinate of a storage location is negative TRPROG will read the data from the further plane. When the x coordinate is positive TRPROG will read the data from the closer plane, (see figure 4).

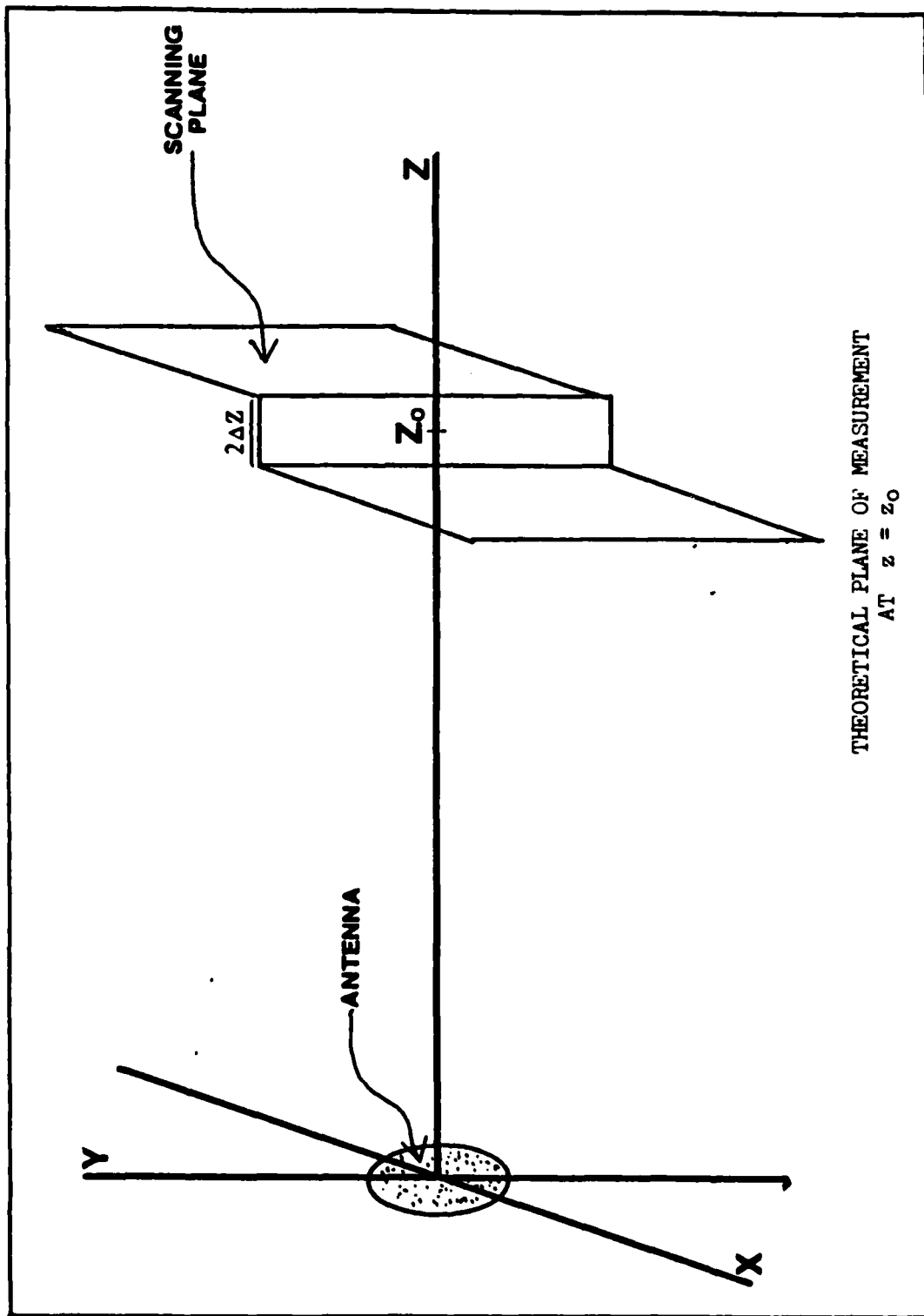


Figure 4. Modeled Probe Positioning Errors.

This is a convenient model for positioning errors due to its ease of implementation and due to the predictability of the effects these errors will have on the far-field patterns.

For small displacements at the y-axis, the magnitude difference between the two halves comprising the near-field data will be negligible. The phase difference created by propagation will not, however, be negligible (17:24). This system can be approximated by a two element linear array, and the theory of linear arrays leads one to expect a shift in the position of the main beam. Indeed, this shift is observed in the computation of the far-field patterns.

V. THE DATA

This chapter will present the data produced by the correction routine. Included is a discussion of the validity of the simulation used to model probe positioning errors, as well as an evaluation of the performance of the transformational programs, TRPROG, and DRPROG.

The Model

As outlined in chapter IV, the model used to simulate erroneous probe positioning consists of a discrete jump, equal to $2\Delta z$, in the measurement plane at the y-axis (see figure 4). It can be argued that this is not a realistic simulation of the positioning errors found in an actual measurement facility. While this is true, the errors represented by this model are, most probably, more severe than those of a real near-field system. Thus, if these exaggerated errors do not present undo difficulties to the correction procedure, the program can reasonably be expected to perform at least as well when confronted with the, relatively, benign inaccuracies of a high precision near-field measurement system.

The only limitation presented by this particular correction routine is that the mean z position of the probe be equal to the theoretical measurement plane $z=z_0$. This ensures a proper phase reference for the far-field pattern.

Computation Procedure

The general procedure for the computation of a corrected far-field pattern is outlined in chapter III, figure 2. The presentation of the data for comparison, however, requires that the far-field pattern be computed neglecting any positioning errors. This is accomplished by supplying the program OUTPROG with the raw data before it is processed by the correction routine. The generation of a complete set of data that facilitates the comparison of the corrected, and uncorrected patterns is outlined in figure 5.

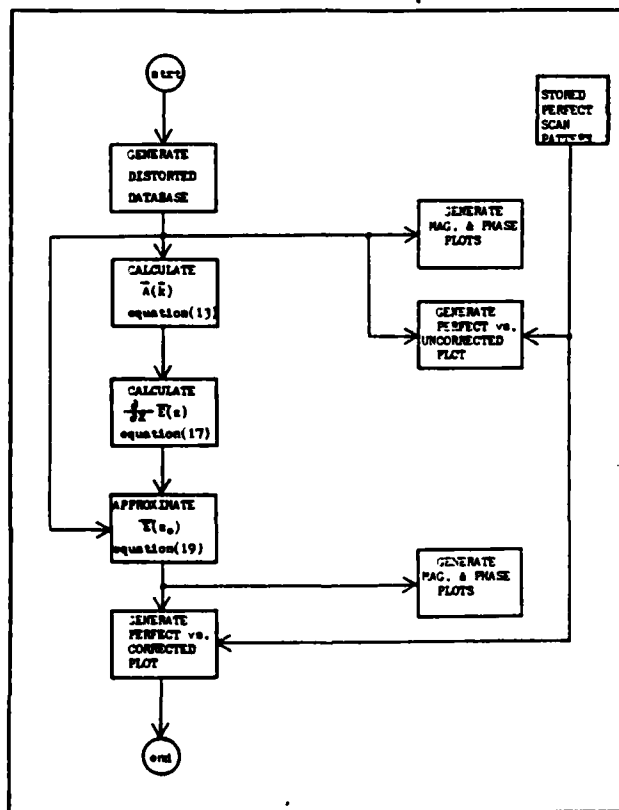


Figure 5. Computation Procedure for Data Presentation.

Data Presentation

The computer simulation was performed for an antenna whose diameter is two meters and is operating at 2.4 GHz. Data sets were generated for two values of the parameter z . The first set, shown in figures 6 and 7, is for a positioning error of $\lambda/25$ (5 mm). Figure 6, shown below, is a comparison plot of the far-field pattern computed from a perfect scan (i.e. no positioning errors), versus the plot of the far-field pattern computed from a scanning plane distorted as shown in figure 4. The plot is of a cut made along the $\phi = \pi/4$ contour. The main lobe has been shifted by approximately $1/3$ degree.

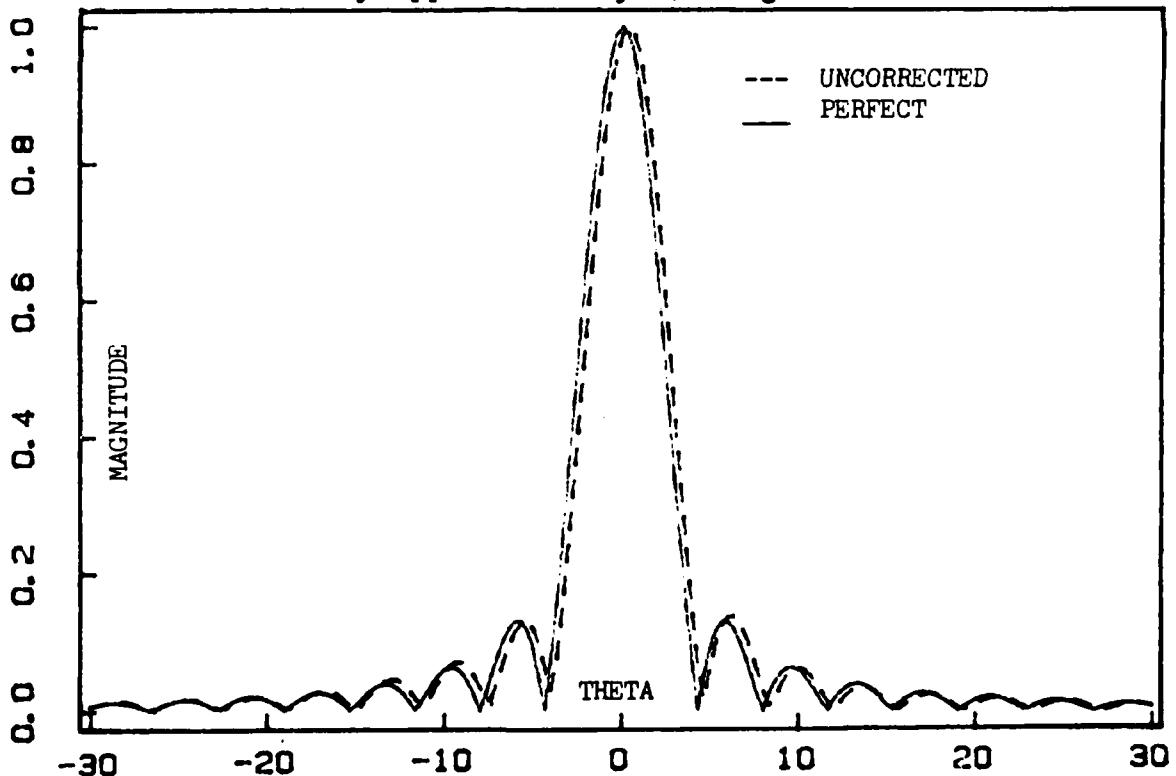


Figure 6. Perfect Scan Pattern vs. Uncorrected Pattern.
 $z = \lambda/25$

The shift in the main lobe closely matches the shift predicted for a two element, linear array. The theoretical shift, along the $\phi = \pi/4$ cut line is given by:

$$\Delta\theta = \sin^{-1}\left(\frac{4\pi/25}{2\pi a/\lambda}\right) \cos(\pi/4) = 0.4^\circ \quad (30)$$

Figure 7 is a plot, made over the same contour, of the far-field pattern of a perfect scan versus the far-field pattern of the corrected scan. It is evident that the main lobe has been moved back towards the undistorted position.

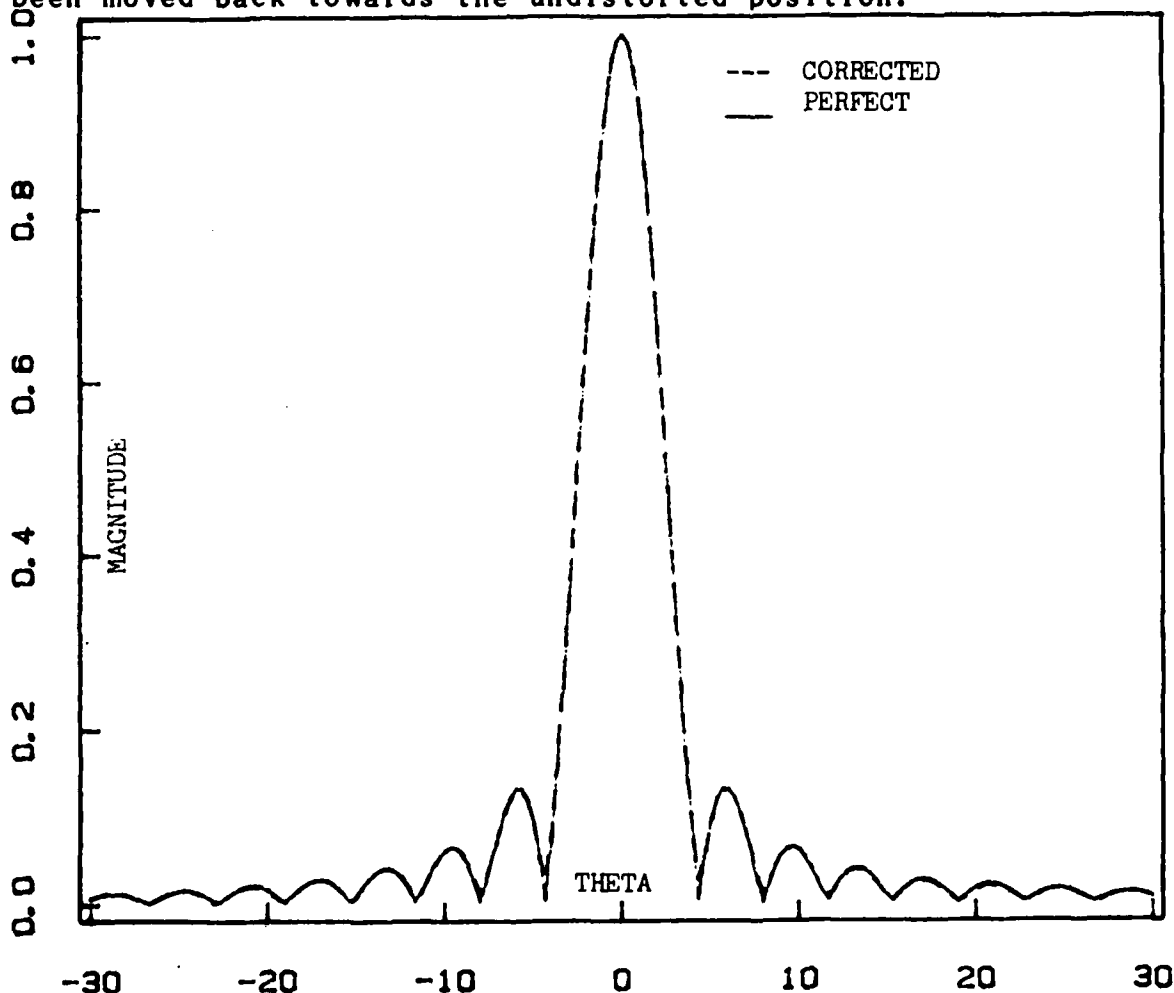


Figure 7. Perfect Scan Pattern vs. Corrected Pattern.
 $\Delta z = \lambda/25$

Figures 8 and 9 are similar plots for $\Delta z = \lambda / 10$ (12.5 mm). Figure 8 shows the effect of the distorted scan, and again the main lobe has shifted away from the z-axis in this case, however, the shift is approximately 1 degree. In this example, the level of the sidelobes has risen slightly.

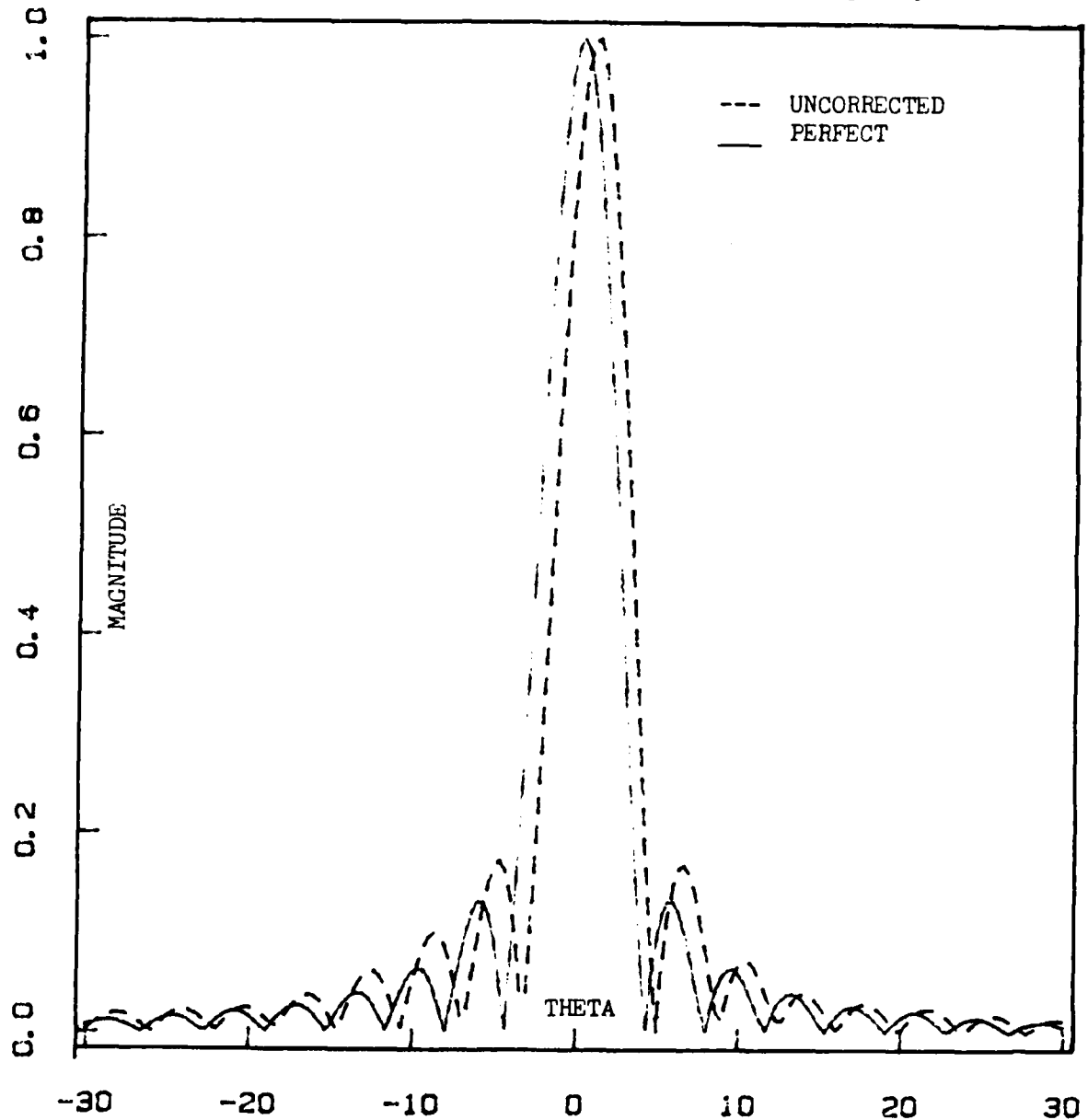


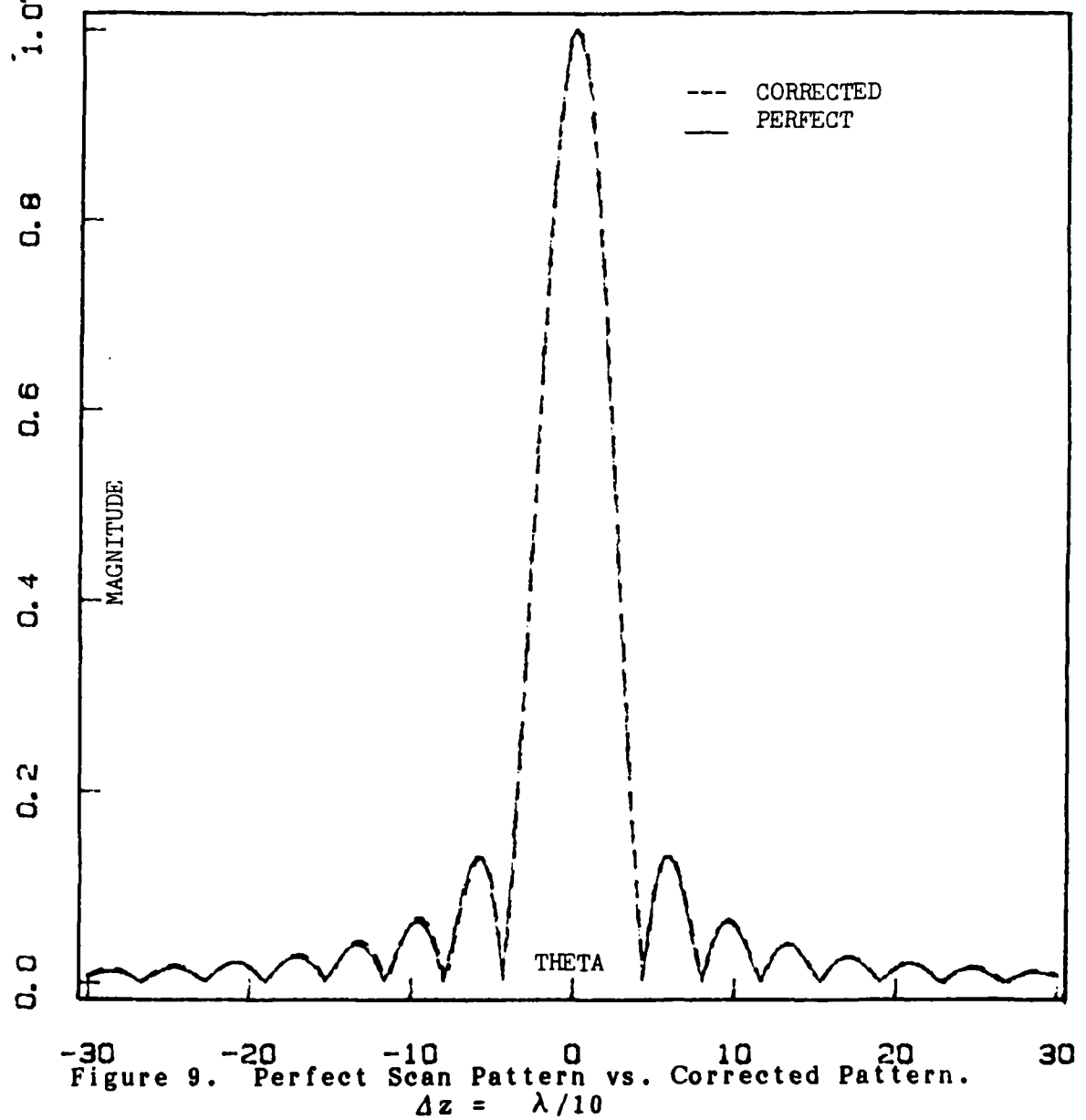
Figure 8. Perfect Scan Pattern vs. Uncorrected Pattern.
 $\Delta z = \lambda / 10$

The predicted shift in the main lobe is given by:

$$\Delta\theta = \sin^{-1}\left(\frac{4\pi/10}{2\pi a/\lambda}\right) \cos\left(\frac{\pi}{4}\right) = 1.01^\circ \quad (31)$$

still very close to the observed shift.

Figure 9 plots the perfect pattern versus the corrected pattern.



To fully understand the correction procedure, one must observe what happens to the near-field magnitude, and phase patterns of the corrected, and uncorrected scans.

Figures 10 and 11 are plots of the corrected and uncorrected phase patterns of the near-field scans. Figure 10 is a cut of the near-field phase distribution as the probe moves in the x direction on the distorted scan surface vs. the same cut made on the perfect scan. Note that the jump in phase across the origin is due to the distorted scanning plane.

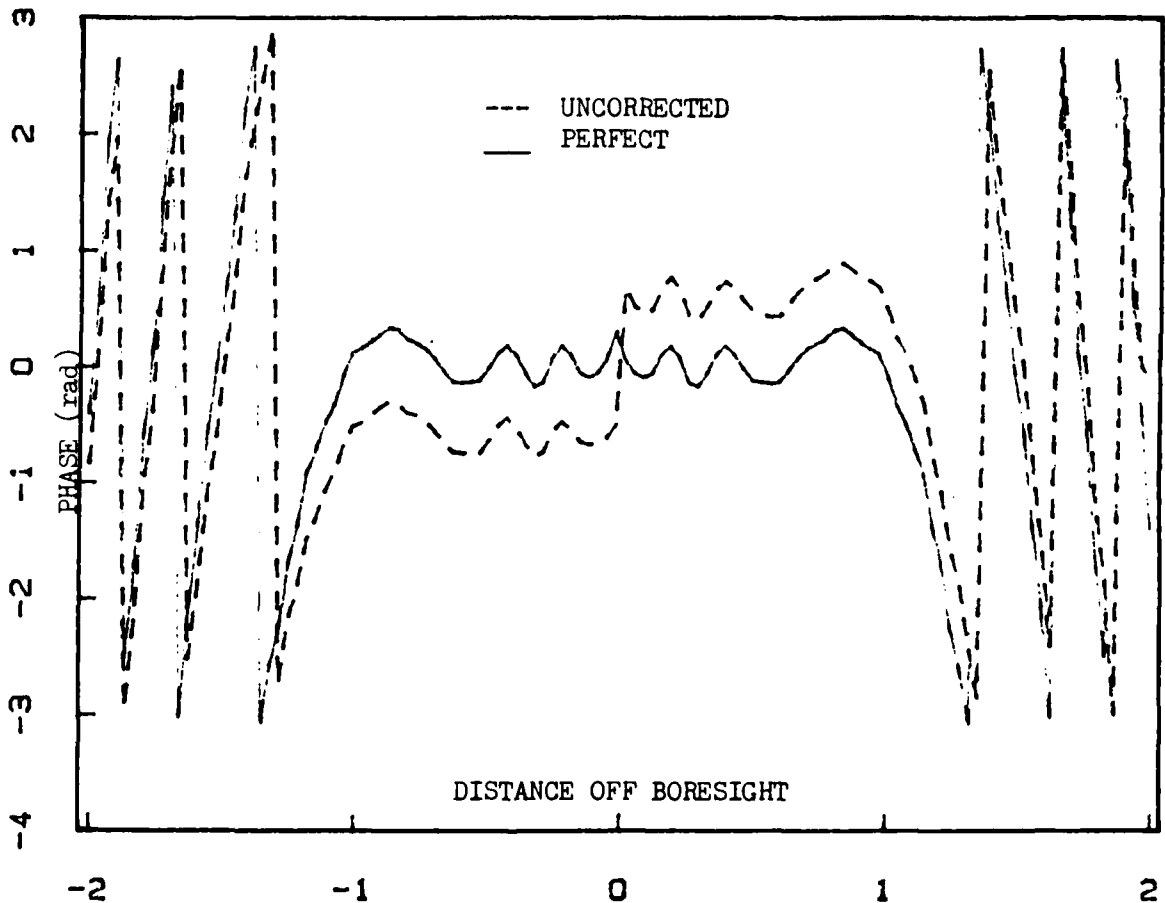


Figure 10. Near-Field Phase, Uncorrected Scan.
 $\Delta z = \lambda / 10$

Figure 11 shows the effect of the correction procedure. The phase jump at the origin has been reduced to a negligible value and the phase is, roughly constant across the face of the antenna. Since the theoretical scanning plane was taken to be an integral number of wavelengths, $z_0 = 1.125$ m, the approximate 0° phase across the main beam of the near-field, shown below, is expected.

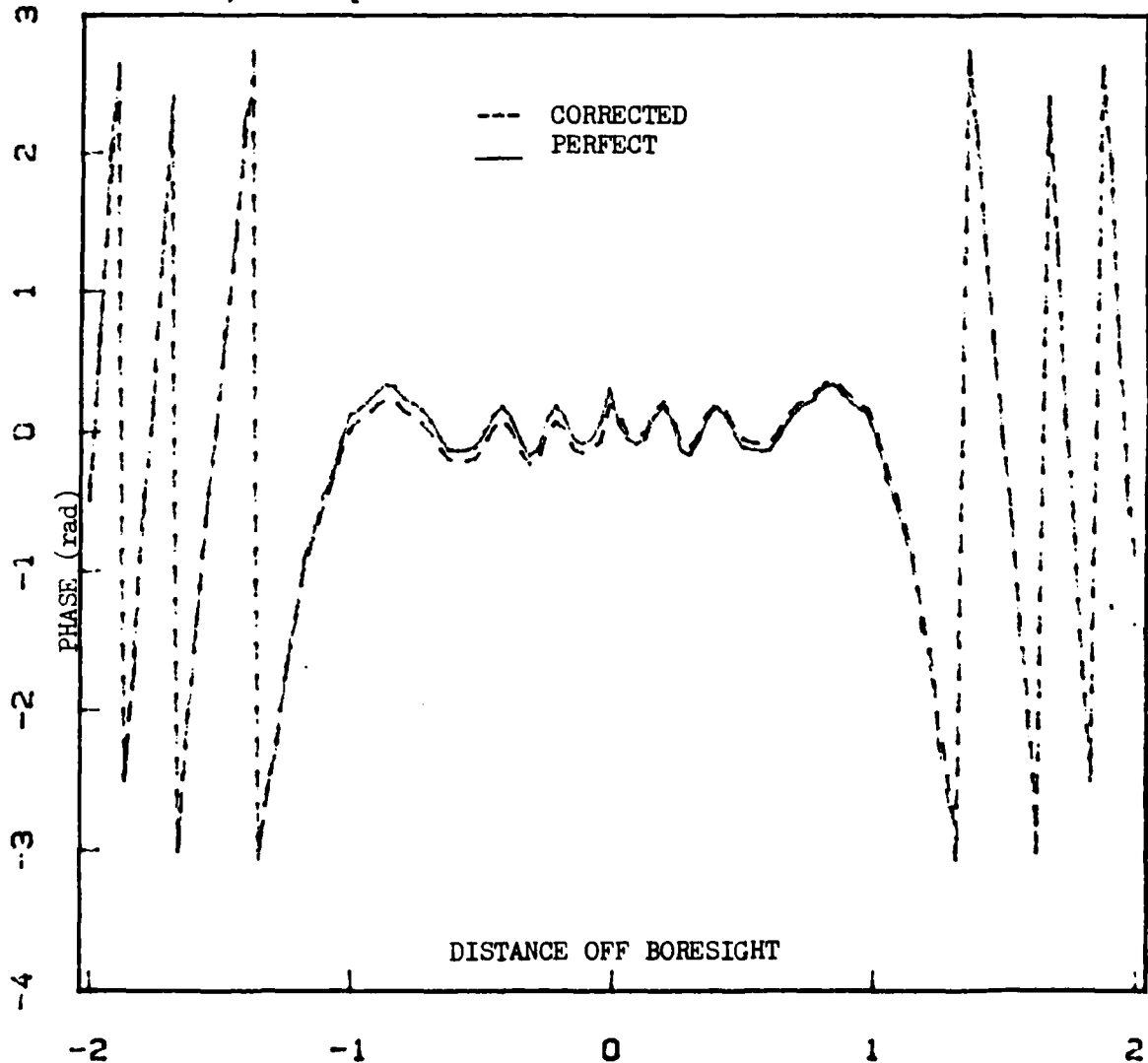


Figure 11. Near-Field Phase, Corrected Scan.
 $\Delta z = \lambda / 10$

Figures 12 and 13 are plots of the magnitude distributions in the x direction on the distorted scan surface. Figure 12 is the magnitude pattern of the near-field scan before the implementation of the correction routine.

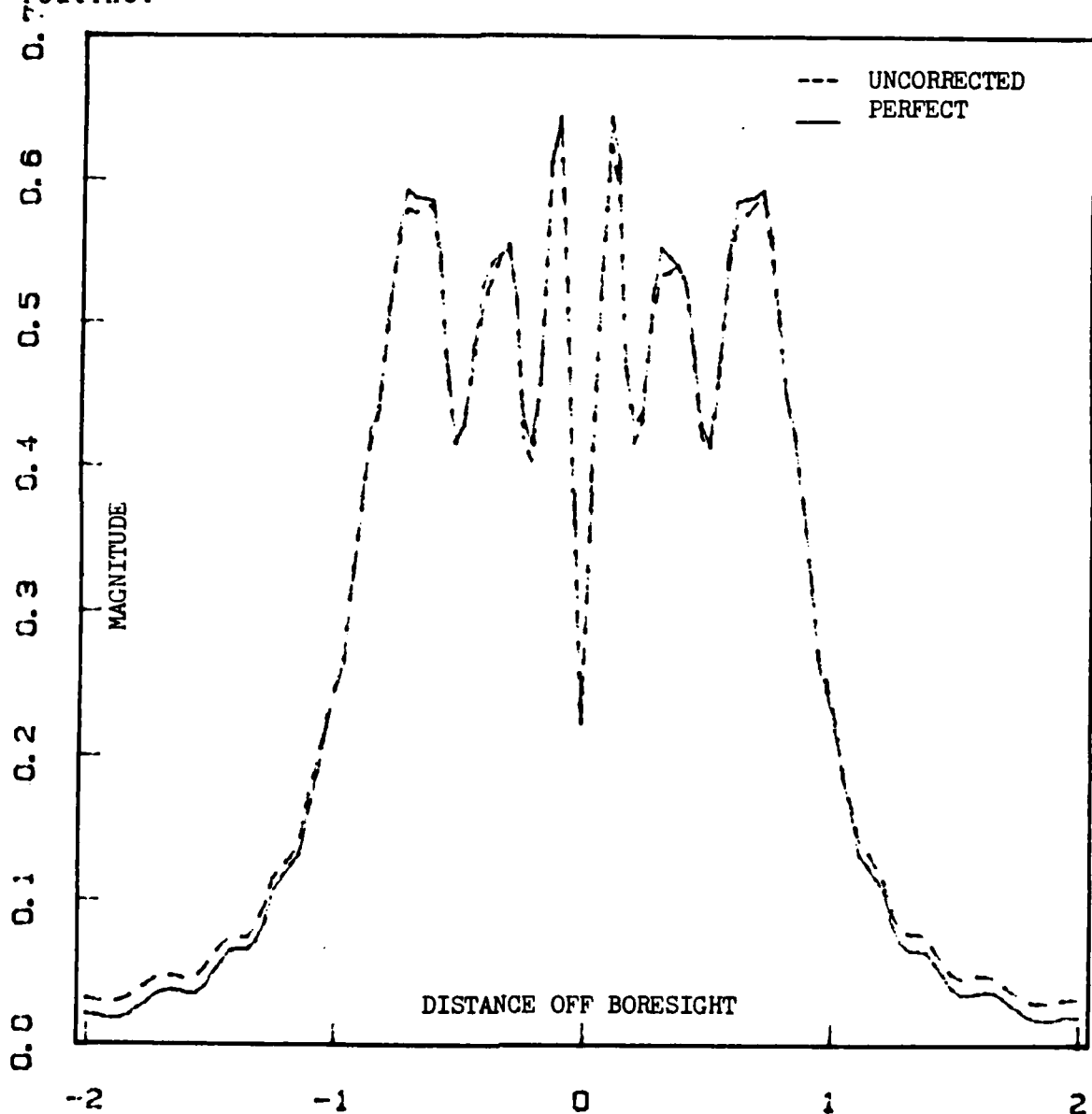


Figure 12. Near-Field Magnitude, Uncorrected Scan.
 $\Delta z = \lambda/10$

In figure 13 the corrected magnitude pattern is shown, again as the probe moves in the x direction along the distorted scan surface vs. the same contour on the perfect scan. It can be seen that the pattern differs from the uncorrected scan in that the curve appears to follow the perfect scan slightly more closely with the exception of a constant shift for all values over the main beam of the near-field pattern. Since the far-field patterns calculated from this data were normalized with respect to the main beam, this constant shift does not seriously affect the far-field patterns.

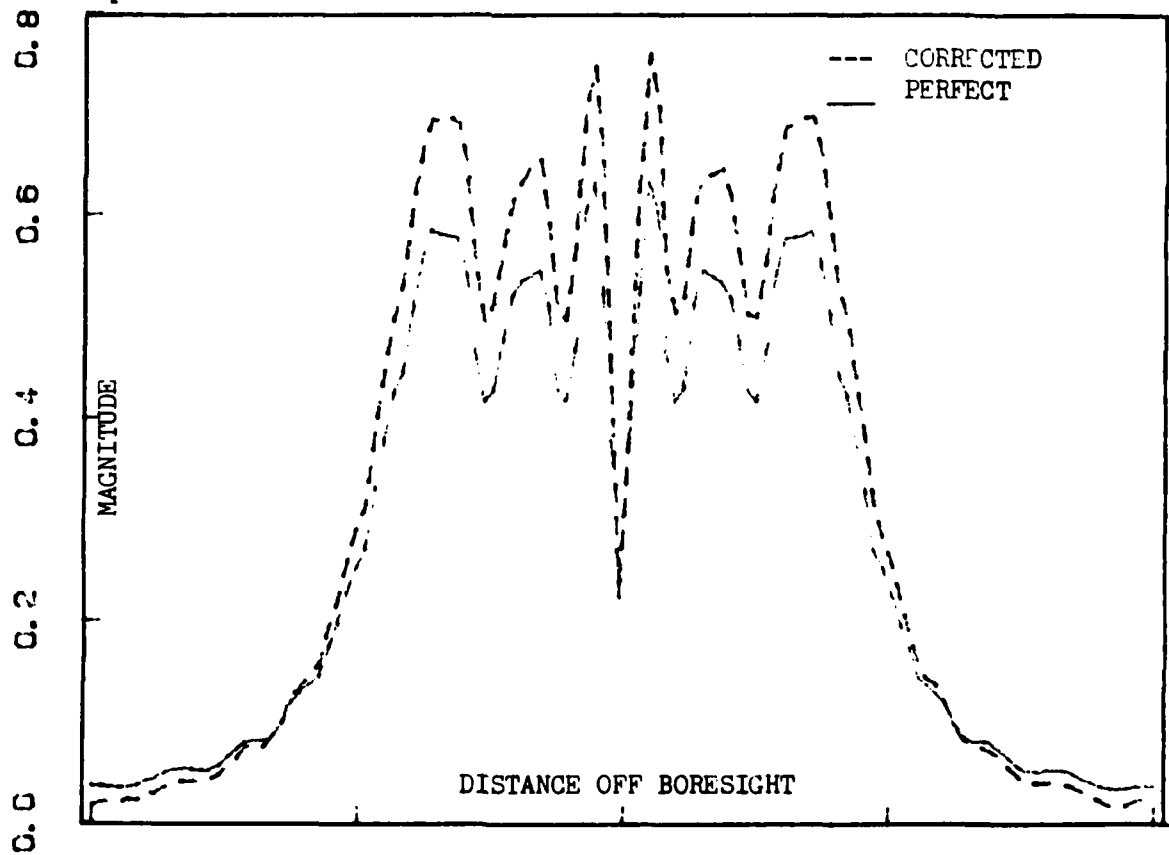


Figure 13. Near-Field Magnitude, Corrected Pattern.
 $\Delta z = \lambda/10$

Evaluation of the Programs

There are two main components of the transformation, and correction process, the program TRPROG, and the program DRPROG. Both routines share a common disadvantage in that a complete grid of data must be computed in order to implement the correction routine. This is due to the fact that, for this model, positioning error corrections must be performed for each point. The consequence of this is that the computation time is greatly extended. This could be avoided by using a more efficient transformation algorithm, such as a Fast Fourier Transform, and setting some tolerance threshold, that is only correct those measurements that are determined to be excessively inaccurate. This can be done using these techniques since the correction procedure is point by point in nature. In this way, the derivative of the near-field values would only have to be computed at the points where it is needed most.

Another point to consider, is the accuracy of the presented data. The far-field patterns were computed at increments of $\theta = 1/3$ degree, then normalized to the largest value computed. In this way some error is introduced into the output. If the actual maximum of the far-field pattern occurred between two data points, the program would tend to mask the fact. This data spacing was chosen to expedite the execution time while still providing reliable accuracy. If for a given utilization, the main lobe was all that needed

to be considered, the data spacing could be substantially reduced.

VI. RESULTS AND RECOMMENDATIONS

The main goals of this investigation were accomplished in that the effects of probe positioning errors were investigated and found to be significant, even for errors much less than a wavelength. The viability of the correction routine was investigated and determined to adequately correct the errors introduced by inaccurate probe positioning given that those errors are small in comparison to a wavelength.

At first glance, the cases studied in this report may seem to represent an extreme case of inaccurate probe positioning. This is not the case since the errors were represented with respect to wavelength. If the test antenna had been operating at 30 GHz instead of 2.4 GHz, a positioning error of $\lambda/25$ would represent a distance of 0.4 mm, a very fine tolerance when it has to be maintained over a space of two meters!

The use of this correction routine could reduce the need for extremely accurate, and therefore expensive, positioners without sacrificing reliable far-field patterns. Several questions remain to be answered, however, before this routine could be implemented. What is the relationship between the correction routine, and errors in the magnitude distribution of the corrected near-field scan? Is the correction routine responsible for the magnitude errors, or are they due to the crude integration algorithms used?

Can the routines be modified so that they can be used in conjunction with scanning geometries other than planar?

Along with these technical questions, there are several problems involved in the application, and optimization of this procedure. The programs need to be reworked using a more efficient Fourier transformation algorithm. Probe correction needs to be taken into consideration. The problem of the presence of noise in a real data set needs to be investigated. These questions represent a valuable source of research opportunities which require detailed investigations and could lead to follow on theses for future AFIT students.


```

CALL SPHEBE(-(LMAX+1)/2,XKWA/2.,RES,XJMK2)
CALL FACT(LMAX,XF,F)
CALL FCFAC((2*LMAX-1),XFF,FF)

```

C
C
C
C
C
C
C

THIS ROUTINE COMPUTES THE SUMMATION CONSTANT, BL

IF(LMAX.LT.1) GO TO 100

C

```

DO 20 L1=1,LMAX,2
L=L1-1
LO2=L/2
SQP=(FF(L+1)/F(LO2+1)*XJKAO2(1))**2*(-1)**LO2
IF(L-1)40,40,50
CONTINUE
IF(LO2.LT.1) GO TO 105

```

50

C

```

DO 30 IQP=1,LO2
F1=FF(L+1-2*IQP)/F(LO2-IQP+1)
F2=FF(L+1+2*IQP)/F(LO2+IQP+1)
ISUB=IQP+1
FJ=XJKAO2(ISUB)*XJMK2(ISUB)
QP=2.*F1*F2*FJ*(-1)**(LO2+IQP+2)
SQP=SQP+QP
CONTINUE

```

30

C

105

CONTINUE

40

CONTINUE

BL(L1)=(2.*L+1)/2.**(L+1.)*SQP

20

CONTINUE

100

CONTINUE

C

C

```

DO 200 IKRT=1,501
XKRT=MKR*(IKRT-1.)/500
XKWR=SQRT(XKRT**2+ZK**2)
THETA=ACOS(ZK/XKWR)
CALL SPHEBE(LMAXP1,XKWR,RES,XJKR)
CALL SPHEBE(-LMAXP1,XKWR,RES,XNKR)
IF(LMAXP1.LT.1) GO TO 115

```

C

```

DO 10 I=1,LMAXP1
XNKR(I)=XNKR(I+1)*(-1)**I
CONTINUE

```

10

C

115

```

CONTINUE
CALL LEGEND(LMAXP1,THETA,PLL,PL)
SUM1=0.
SUM2=0.
IF(LMAX.LT.1)GO TO 120

```

```

C
DO 90 L1=1,LMAX,2
  L=L1-1
  TL11=L1*(ZK/XKWR*PL(L1)-PL(L1+1))*XJKR(L1)
  TL12=(L*XJKR(L1)-XKWR*XJKR(L1+1))*PL(L1)
  CSTHTA=ZK/XKWR
  TL12=TL12*CSTHTA
  SUM1=(TL11+TL12)*BL(L1)+SUM1
  TL21=L1*(ZK/XKWR*PL(L1)-PL(L1+1))*XNKR(L1)
  TL22=(L*XNKR(L1)-XKWR*XNKR(L1+1))*PL(L1)
  TL22=TL22*CSTHTA
  SUM2=(TL21+TL22)*BL(L1)+SUM2
90  CONTINUE
C
120  CONTINUE
  COEF=.5*XKWA**2/XKWR
  P=COEF*SQRT(SUM1**2+SUM2**2)
  PN(IKRT)=P
  PNLOG(IKRT)=20.*ALOG10(PN(IKRT))
  PKROKZ(IKRT)=P*XKWR/ZK
  PHASE(IKRT)=ATAN2(SUM2,SUM1)
200  CONTINUE
C
      OPEN(UNIT=10,FILE='DAT2')
C
      DO 18 I=1,501
      XI=(3./500.)*(I-1.)
      WRITE(10,17) PHASE(I),PN(I)
18    CONTINUE
C
17    FORMAT(E20.7,10X,E20.7)
      ENDFILE 10
      CLOSE(UNIT=10)
      STOP
      END
      SUBROUTINE FACT(N,F,FMTRX)
C      THIS ROUTINE COMPUTES 0 TO N FACTORIAL, AND STORES
C      IN THE MATRIX, FMTRX
C
      DIMENSION FMTRX(500)
      FMTRX(1)=1.0
      IF(N)11,11,20
20    IF (N.LT.1) GO TO 100
C
      DO 10 I=1,N
      FMTRX(I+1)=FMTRX(I)*I
10    CONTINUE
C
100  CONTINUE
11    CONTINUE
      F=FMTRX(N+1)
      RETURN

```

```

11 CONTINUE
   F=FMTRX(N+1)
   RETURN
   END
   SUBROUTINE FCFAC(N,FF,FFMAT)
C   COMPUTES THE FIRST N FAC-FACTORIAL AND STORES IN FFMAT
C
   DIMENSION FFMAT(1000)
   FFMAT(1)=1.0
   IF(N)11,11,20
20  IF(N.LT.1)GO TO 100
C
      DO 10 I=1,N,2
      FFMAT(I+2)=FFMAT(I)*I
10  CONTINUE
C
100 CONTINUE
11  CONTINUE
   FF=FFMAT(N+2)
   RETURN
   END
   SUBROUTINE SPHEBE(LEL,X,RESULT,T)
C   COMPUTES SPHERICAL J OF ORDER 0 TO LEL AND STORES IN
C   T
C
   DIMENSION T(2500)
1  IF(X)18,12,18
12  IF(LEL)16,13,14
13  RESULT=1.0
   T(1)=RESULT
   RETURN
14  RESULT=0.0
   T(1)=1.0
   LELP1=LEL+1
   IF(LELP1.LT.2) GO TO 100
C
      DO 40 I=2,LELP1
      T(I)=0.0
40  CONTINUE
C
100 CONTINUE
   RETURN
16  RESULT=1.0E+300*(-1)**(LEL+1)
   T(1)=1.0
   MI=-LEL+1
   IF(MI.LT.1) GO TO 105
C
      DO 30 I=2,MI
      T(I)=1.0E+300*(-1)**I
30  CONTINUE
105 CONTINUE
   RETURN

```

```

18   IF(LEL)55,51,19
19   MO=LEL
      JO=2*IFIX(X)
      IF(MO-JO)2,21,21
2    MO=JO
21   MO=MO+11
22   T(MO)=0.
      T(MO-1)=1.0E-285
      LO=MO-2
23   F=2*(MO-1)
231  MO=MO-3
      I2=MO
232  F=F-2.0
      T(I2+1)=(F+1.)/X*T(I2+2)-T(I2+3)
      IF(I2)4,3,4
4    I2=I2-1
      GO TO 232
3    F=SIN(X)/X/T(1)
      IF(MO.LT.1)GO TO 110
C
      DO 5 J=1,MO
5    T(J)=F*T(J)
C
110  CONTINUE
      RESULT=T(LEL+1)
      RETURN
51   RESULT=SIN(X)/X
      T(1)=RESULT
      RETURN
55   LO=-LEL+1
      T(1)=SIN(X)/X
      T(2)=COS(X)/X
      IF(LO.LT.3)GO TO 115
C
      DO 6 J=3,LO
6    T(J)=(-2.*FLOAT(J-2)+1)/X*T(J-1)-T(J-2)
C
115  CONTINUE
      RESULT=T(LO)
      RETURN
      END
      SUBROUTINE LEGEND(N,THETA,P,PMTRX)
C    COMPUTES LEGEND POLY OF ORDER 0 TO N AND STORES IN PMTRX
C
      DIMENSION PMTRX(500)
      X=COS(THETA)
      PMTRX(1)=1.0
      PMTRX(2)=X
      NP1=N+1
      IF(N-1)10,10,11
11   CONTINUE
      IF(NP1.LT.3)GO TO 100

```

```
C      DO 20 I=3, NP1
      XI=1
      PMTRX(I) = ((2.*XI-3.)*X*PMTRX(I-1) - (XI-2.)*
+      PMTRX(I-2)) / (XI-1.)
20    CONTINUE
C
100   CONTINUE
10    CONTINUE
      P=PMTRX(NP1)
      RETURN
      END
```

TRPROG

PROGRAM TRPROG

C
C
C
C
C
C
C

THIS PROGRAM IS DESIGNED TO CALCULATE THE FAR-FIELDS
ANTENNA PATTERNS OF AN ARBITRARY TEST ANTENNA, FROM
THE NEAR-FIELD VALUES ON A SCANNING PLANE A
SPECIFIED DISTANCE FROM THE ANTENNA

REAL PHS1(550)
REAL PHS2(550)
REAL PN1(550)
REAL PN2(550)
REAL KO
COMPLEX EX1(151,151)
COMPLEX A1(100,100)
COMPLEX SM(155,100)
COMPLEX XI,XMI
COMPLEX CSUM
COMPLEX KT
COMPLEX KZ
REAL DELTAZ
REAL ZO
REAL LAMBDA
REAL KA

C

LAMBDA=1.0/8.0
PI=4.*ATAN(1.)
DELTAZ=.005
ZO=1.125
XI=(0.,1.)
XMI=(0.,-1.)
KO=2*PI/LAMBDA
DK=(1.0/40.0)*KO
DX=4/116.0

C
C
C
C
C
C
C
C

THIS LOOP WILL READ IN THE NEAR-FIELD DATA

OPEN(UNIT=10,FILE='DAT1')
OPEN(UNIT=9,FILE='DAT2')
REWIND(UNIT=10)
REWIND (UNIT=9)

```

C          DO 12 I=1,501
          READ(10,17) PHS1(I),PN1(I)
          READ(9,17) PHS2(I),PN2(I)
12         CONTINUE
C
17        FORMAT( E20.7,10X,E20.7)
          CLOSE(UNIT=10)
          CLOSE(UNIT=9)
C
          DO 45 I=1,117
C
          DO 40 J=1,117
          JL=J-1
          IL=I-1
          R=SQRT((-2+JL*DX)**2+(-2+IL*DX)**2.)
          IQ=INT(R*1000.)-10*INT(100.*R)
          TNR=500./3.
          IF(IQ.GE.5) IR=INT(R*TNR+1)
          IF(IQ.LT.5) IR=INT(R*TNR)
          IR=IR+1
          IF(JL*DX-2.LE.0.0)GOTO 37
          ER=PN1(IR)*COS(PHS1(IR))
          EI=PN1(IR)*SIN(PHS1(IR))
          GO TO 39
37         ER=PN2(IR)*COS(PHS2(IR))
          EI=PN2(IR)*SIN(PHS2(IR))
39         EX1(J,I)=CMPLX(ER,EI)
          OPEN(UNIT=10,FILE='NDAT')
          WRITE(10,117) REAL(EX1(J,I)),AIMAG(EX1(J,I))
117        FORMAT( E20.7,1X,E20.7)
          CONTINUE
C
45        CONTINUE
C
C          THIS LOOP CALCULATES THE APPROXIMATE VECTOR AMPLITUDE
C          USED IN THE DDZEX1 ROUTINE
C
C
C
C
C
C
          DO 60 I=1,81
C
          DO 55 J=1,117
          CSUM=(0.,0.)
C
          DO 50 M=1,117
          KA=(-2+(M-1)*DX)*(-KO+(I-1)*DK)
          KT=CMPLX(0.,KA)
          CSUM=CSUM+EX1(M,J)*CEXP(KT)
          *DX**2.
+

```

```

50          CONTINUE
C
          SM(J,I)=CSUM
55          CONTINUE
C
60          CONTINUE
C
          DO 75 I=1,81
C
          DO 70 J=1,81
          CSUM=(0.,0.)
C
          DO 65 M=1,117
          KA=(-KO+(J-1)*DK)**2.+(-KO+(I-1)*DK)**2.
          IF(KA.GT.KO**2) GO TO 65
          IF(KA.LE.KO**2)KZ=SQRT(KO**2-KA)
          KT=CMPLX(0.,(-2+(M-1)*DX)*(-KO+(I-1)*DK))
          KT=KT+KZ*ZO*X1
          CSUM=CSUM+SM(M,J)*
+          CEXP(KT)/(2.*PI)
65          CONTINUE
C
          A1(J,I)=CSUM
          OPEN(UNIT=7,FILE='FRST')
          WRITE(7,150) REAL(A1(J,I)),AIMAG(A1(J,I))
70          CONTINUE
C
75          CONTINUE
C
150         FORMAT( E20.7,1X,E20.7)
C
          STOP
          END

```



```

17   FORMAT( E20.7,1X,E20.7)
C
    CLOSE(UNIT=7)
C
C
C   THIS LOOP WILL CALCULATE THE ACTUAL DERIVATIVE
C
C   DO 30 I=1,117
C
C       DO 25 J=1,81
C           CSUM=(0.,0.)
C
C               DO 20 M=1,81
C                   ML=M-1
C                   IL=I-1
C                   JL=J-1
C                   KA=(ML*DK-KO)**2.+(JL*DK-KO)**2.
C                   IF(KA.GT.(.75)*KO**2.) GOTO 20
C                   IF(KA.LE.(.75)*KO**2.) KZ=SQRT(KO**2.-KA)
C                   KX=CMLPX(0.,-(IL*DX-2)*(ML*DK-KO))
C                   KT=KX+KZ*ZO*XMI
C                   CSUM=CSUM+A1(M,J)*XMI*KZ*CEXP(KT)/(2.*PI)
C                   CONTINUE
20
C
C           SM(I,J)=CSUM
C           CONTINUE
25
C
C       CONTINUE
30
C
C   DO 45 I=1,117
C
C       DO 40 J=1,117
C           CSUM=(0.,0.)
C
C               DO 35 M=1,81
C                   ML=M-1
C                   IL=I-1
C                   KY=CMLPX(0.,-(ML*DK-KO)*(IL*DX-2))
C                   CSUM=CSUM+SM(J,M)*CEXP(KY)*DK**2.
35
C
C           DDZEX1=CSUM
C           OPEN(UNIT=9,FILE='THRD')
C           WRITE(9,100) REAL(DDZEX1),AIMAG(DDZEX1)
40
C
C       CONTINUE
45
100  FORMAT( E20.7,1X,E20.7)
    STOP
    END

```

COMPROG

PROGRAM COMBN

C
C
C
C
C
C
C
C

THIS PROGRAM WILL COMBINE THE ORIGINAL NEAR-FIELD DATA,
WITH THE CALCULATED DERIVATIVE OF THE NEAR-FIELD DATA,
AND OBTAIN AN APPROXIMATION OF THE NEAR-FIELDS ON THE
THEORETICAL PLANE OF MEASUREMENT.

COMPLEX EX1(155,155)
COMPLEX DDZ(155,155)
COMPLEX EXO
COMPLEX SUM
REAL DER,DEI
REAL DELTAZ,DX
REAL PHS1(550)
REAL PHS2(550)
REAL PN1(550)
REAL PN2(550)

C
C

DELTAZ=(1.0/8.0)*.1
DX=4/116.0

C
C
C
C
C

THIS LOOP WILL READ IN THE NEAR-FIELD DATA

OPEN(UNIT=10,FILE='DAT1')
OPEN(UNIT=9,FILE='DAT2')
REWIND(UNIT=10)
REWIND (UNIT=9)

C

DO 12 I=1,501
READ(10,17) PHS1(I),PN1(I)
READ(9,17) PHS2(I),PN2(I)
CONTINUE

12

C

17

FORMAT(E20.7,10X,E20.7)
CLOSE(UNIT=10)
CLOSE(UNIT=9)

C

C

DO 45 I=1,117

DO 40 J=1,117
JL=J-1
IL=I-1
R=SQRT((-2+JL*DX)**2.+(-2+IL*DX)**2.)

```

      IQ=INT(R*1000.)-10*INT(100.*R)
      TNR=500./3.
      IF(IQ.GE.5)IR=INT(R*TNR+1)
      IF(IQ.LT.5)IR=INT(R*TNR)
      IR=IR+1
      IF(JL*DX-2.LE.0.0)GOTO 37
      ER=PN1(IR)*COS(PHS1(IR))
      EI=PN1(IR)*SIN(PHS1(IR))
      GO TO 39
37      ER=PN2(IR)*COS(PHS2(IR))
      EI=PN2(IR)*SIN(PHS2(IR))
39      EX1(J,1)=CMPLX(ER,EI)
      OPEN(UNIT=8,FILE='NDAT')
      WRITE(8,35) REAL(EX1(J,1)),AIMAG(EX1(J,1))
      CLOSE(UNIT=8)
40      CONTINUE
C
45      CONTINUE
C
C      THIS LOOP WILL READ IN THE FIRST DERIVATIVE.
C
C
      OPEN(UNIT=9,FILE='THRD')
      REWIND(UNIT=9)
C
      DO 15 J=1,117
C
          DO 10 I=1,117
          READ(9,21) DER,DEI
          DDZ(I,J)=CMPLX(DER,DEI)
10          CONTINUE
C
15          CONTINUE
C
          CLOSE(UNIT=9)
21          FORMAT( E20.7,1X,E20.7)
C
C      THIS LOOP WILL COMBINE EX1(X,Y) AND DDZ(X,Y)
C
C
      DO 25 J=1,117
C
          DO 20 I=1,117
          IL=I-1
          IF((IL*DX-2).LE.0.0) GO TO 18
          SUM=EX1(I,J)-DELTAZ*DDZ(I,J)
          GO TO 19
18          SUM=EX1(I,J)+DELTAZ*DDZ(I,J)
19          EXO=SUM
          OPEN(UNIT=7,FILE='EXOUT')

```

```
20      WRITE(7,35) REAL(EXO),AIMAG(EXO)
C      CONTINUE
25      CONTINUE
C
35      FORMAT( E20.7,1X,E20.7)
STOP
END
```

OUTPROG

PROGRAM OTPROG

C
C
C
C
C
C
C

THIS PROGRAM WILL CALCULATE THE FAR-FIELD PATTERN
OF THE TEST ANTENNA AND PRESENT THE MATERIAL IN A
FORM SUITABLE FOR VIEWING.

COMPLEX EXO(155,155)
COMPLEX AO(375)
COMPLEX KA
COMPLEX CSUM
COMPLEX XI
COMPLEX K1,K2
REAL EFF(500)
REAL KX,KY,KZ,DX,PI,LAMBDA,KO,PHI,DT,ZO
REAL ER(155,155),EI(155,155)

C
C
C
C

INITIALIZATION

DX=4/116.0
BIG=0.0
PI=4.0*ATAN(1.0)
LAMBDA=1.0/8.0
KO=2.0*PI/LAMBDA
ZO=1.125
XI=(0.,1.0)
PHI=PI/4.0
DT=PI/540

C
C
C
C
C

THIS LOOP WILL READ IN THE NEAR-FIELD DATA

OPEN(UNIT=7,FILE='SCND')
REWIND(UNIT=7)

C
C

DO 12 I=1,117

C
11
C

DO 11 J=1,117
READ(7,17) ER(J,I),EI(J,I)
EXO(J,I)=CMLX(ER(J,I),EI(J,I))
CONTINUE

12
17

CONTINUE
FORMAT(E20.7,1X,E20.7)
CLOSE(UNIT=7)

C
C
C
C
C

CALCULATE THE OUTPUT OF THE THESIS!!!!!!

DO 30 M=1,181
ML=M-1
CSUM=(0.,0.)

C

DO 25 I=1,117
IL=I-1

C

DO 20 J=1,117
JL=J-1
KX=KO*COS(PHI)*SIN(ML*DT-(PI/6.))
KY=SIN(PHI)*(KX/COS(PHI))
KZ=KO*COS(ML*DT-(PI/6.))
K1=XI*KX*(JL*DX-2.)
K2=XI*KY*(IL*DX-2.)
KA=KZ*XI*ZO+K1+K2
CSUM=CSUM+EXO(J,I)*CEXP(KA)*DX**2./(2.*PI)
CONTINUE

20

C

25

C

CONTINUE

AO(M)=CSUM
EF1=CABS(AO(M))
EF2=CABS(AO(M))*KX/KZ
EFF(M)=SQRT(EF1**2+EF2**2)
IF(BIG.LE.EFF(M))BIG=EFF(M)
CONTINUE

30

C

C

C

C

C

LETS OUTPUT SHALL WE?

DO 35 M=1,181
ML=M-1
THETA=FLOAT(ML)*(1./3.)-30.
OPEN(UNIT=10,FILE='LAST')
WRITE(10,100) THETA,EFF(M)/BIG
CONTINUE
35
100
FORMAT(E20.7,1X,E20.7)
STOP
END

BIBLIOGRAPHY

1. Harrington, Roger F. Time-Harmonic Electromagnetic Fields. New York: McGraw Hill Book Company, 1961.
2. Thiele, Gary A. and Stutzman, Warren L. Antenna Theory and Design. New York: John Wiley & Sons, 1981.
3. Johnson, Richard C. and others. "Determination of Far-Field Antenna Patterns from Near-Field Measurements," Proceedings of the IEEE, 61 (12): 1668-1694 (December 1973).
4. Joy, Edward B. and others. "Applications of Probe-Compensated Near-Field Measurements," IEEE Transactions on Antennas and Propagation, AP-26 (3): 379-389 (May 1978).
5. Paris, Demetrius T. and others. "Basic Theory of Probe-Compensated Near-Field Measurements," IEEE Transactions on Antennas and Propagation, AP-26 (3): 373-379 (May 1978).
6. Joy, Edward B. and Paris, Demetrius T. "Spatial Sampling and Filtering in Near-Field Measurements," IEEE Transactions on Antennas and Propagation, AP-20 (3): 253-261 (May 1972).
7. Yaghjian, Arthur D. "An Overview of Near-Field Antenna Measurements," IEEE Transactions on Antennas and Propagation, AP-34 (1) (January 1986).
8. Yaghjian, Arthur D. "The Fields of a Piston Radiator," Personal Notes. Electromagnetic Sciences Division USAF, Rome Air Development Center, Hanscom AFB, Boston MA.
9. Kummer, Wolfgang H. and Gillespie, Edmond S. "Antenna Measurements-1978," Proceedings of the IEEE, 66 (4): 483-507 (April 1978).
10. Kerns, David M. "Scattering-Matrix Description and Near-Field Measurements of Electroacoustic Transducers," Journal of the Acoustics Society of America, 57 (2): 497-507 (February 1975).
11. Wacker, Paul F. "Unified Theory of Near-Field Analysis and Measurement: Nonmathematical Discussion," IEEE Transactions on Antennas and Propagation, AP-30 (1): 99-107 (January 1982).

12. Kerns, David M. "Plane-Wave Scattering-Matrix Theory of Antennas and Antenna-Antenna Interactions: Formulation and Applications," Journal of Research of the National Bureau of Standards, 80B (1): 5-51 (January-March 1976).
13. Jordan, Edward C. and Balmain, Keith G. Electromagnetic Waves and Radiating Systems, Englewood Cliffs: Prentice-Hall, Inc.
14. Yaghjian, Arthur D. "Efficient Computation of Antenna Coupling and Fields Within the Near-Field Region," IEEE Transactions on Antennas and Propagation, AP-30 (1): 113-128 (January 1982).
15. Yaghjian, Arthur D. Telephone Interview. Electromagnetic Systems Division USAF, Rome Air Development Center, Hanscom AFB, Boston MA. June-October 1985.
16. Newell, Allen C. Telephone Interview. Electromagnetic Fields Division, National Bureau of Standards, Boulder CO. 9 September 1985.
17. Newell, Allen C. "Planar Near-Field Measurements," Lecture materials distributed in a National Bureau of Standards short course, National Bureau of Standards, Boulder CO. June 1985.
18. Arfken, George. Mathematical Methods for Physicists, Orlando: Academic Press, Inc.

VITA

David R. Reddy was born, in Carlsbad New Mexico, on the 22 of February in 1962. He graduated from Carlsbad High School in 1980, and entered New Mexico State University as a freshman studying electrical engineering. Lt. Reddy received his bachelors degree in electrical engineering with high honors on the 5 of May, 1984. Upon graduation he was commissioned as an officer in the United States Air Force. His first assignment was at the Air Force Institute of Technology where he received his masters degree in electrical engineering. Lt. Reddy is a member of Eta Kappa Nu, Tau Beta Pi, and IEEE. Currently he is working at the Air Force Electronic Warfare Center at Kelly AFB in San Antonio Texas.

UNCLASSIFIED

SECURITY CLASSIFICATION OF THIS PAGE

REPORT DOCUMENTATION PAGE

1a. REPORT SECURITY CLASSIFICATION UNCLASSIFIED			1b. RESTRICTIVE MARKINGS		
2a. SECURITY CLASSIFICATION AUTHORITY			3. DISTRIBUTION/AVAILABILITY OF REPORT Approved for public release; distribution unlimited.		
2b. DECLASSIFICATION/DOWNGRADING SCHEDULE					
4. PERFORMING ORGANIZATION REPORT NUMBER(S) AFIT/GE/ENG/85D-34			5. MONITORING ORGANIZATION REPORT NUMBER(S)		
6a. NAME OF PERFORMING ORGANIZATION School of Engineering		6b. OFFICE SYMBOL (If applicable) AFIT/ENG	7a. NAME OF MONITORING ORGANIZATION		
6c. ADDRESS (City, State and ZIP Code) Air Force Institute of Technology Wright-Patterson AFB, Ohio 45433			7b. ADDRESS (City, State and ZIP Code)		
8a. NAME OF FUNDING/SPONSORING ORGANIZATION		8b. OFFICE SYMBOL (If applicable)	9. PROCUREMENT INSTRUMENT IDENTIFICATION NUMBER		
8c. ADDRESS (City, State and ZIP Code)			10. SOURCE OF FUNDING NOS.		
			PROGRAM ELEMENT NO.	PROJECT NO.	TASK NO.
			WORK UNIT NO.		
11. TITLE (Include Security Classification) See Box 19					
12. PERSONAL AUTHOR(S) David R. Reddy, B.S., 2d Lt, USAF					
13a. TYPE OF REPORT MS Thesis		13b. TIME COVERED FROM _____ TO _____		14. DATE OF REPORT (Yr., Mo., Day) 1985 December	15. PAGE COUNT 66
16. SUPPLEMENTARY NOTATION					
17. COSATI CODES			18. SUBJECT TERMS (Continue on reverse if necessary and identify by block number)		
FIELD	GROUP	SUB. GR.			
09	03		Near-Field Scanning (Planar), Fourier Transform Algorithms		
19. ABSTRACT (Continue on reverse if necessary and identify by block number)					
Title: CORRECTION FOR PROBE-POSITION ERRORS IN PLANAR, NEAR-FIELD SCANNING			Approved for public release LAW 85F 280-1 13 Feb 86 JOHN E. WOLAVER Chief for Research and Professional Development Air Force Institute of Technology (AFIT) Wright-Patterson AFB OH 45433		
Thesis Advisor: Randy Jost, First Lieutenant, USAF Instructor of Electrical Engineering					
20. DISTRIBUTION/AVAILABILITY OF ABSTRACT UNCLASSIFIED/UNLIMITED <input checked="" type="checkbox"/> SAME AS RPT. <input type="checkbox"/> DTIC USERS <input type="checkbox"/>			21. ABSTRACT SECURITY CLASSIFICATION UNCLASSIFIED		
22a. NAME OF RESPONSIBLE INDIVIDUAL Randy Jost, First Lieutenant, USAF			22b. TELEPHONE NUMBER (Include Area Code) 513-255-3576	22c. OFFICE SYMBOL AFIT/ENG	

DD FORM 1473, 83 APR

EDITION OF 1 JAN 73 IS OBSOLETE.

UNCLASSIFIED

SECURITY CLASSIFICATION OF THIS PAGE

4

In recent years, near-field antenna measurement techniques have gained a good deal of acceptance. There are several errors in the computed far-field patterns caused by measurement inaccuracies in the near-field data. This paper deals with deterministic errors introduced by probe-positioning errors in planar, near-field scanning.

By utilizing basic near-field theory, as well as a knowledge of the positioning errors, it is possible to estimate the fields at the correct probe position. A computer program which lessens the effect of probe positioning errors by means of a truncated Taylor series expansion is used to demonstrate this improvement.

To simulate inaccurate probe positioning, a database of calculated near-field values for a linearly polarized, uniformly illuminated, circular aperture was used. Next, the position correction program was applied to computer generated inaccurate data. Finally, far-field patterns were calculated, and compared using both the corrected and uncorrected data. Results of the comparisons are presented. Limitations, and areas of application of this routine are discussed.

(The end)

END
FILMED

5-86

DTIC